VŠB – Technical University of Ostrava
Faculty of Metallurgy and Materials Engineering
Department of Material Engineering

Bachelor Thesis

Investigation of shaft fracture of EPX vacuum pump

Zkoumání lomu hřídele EPX vakuové pumpy

2016

Petr Bílek

VŠB - Technical University of Ostrava
Faculty of Metallurgy and Materials Engineering
Department of Material Engineering

Bachelor Thesis Assignment

Student: **Mgr. Petr Bílek, Ph.D.**

Study Programme: B3923 Materials Engineering

Study Branch: 3911R030 Engineering Materials

Title: Investigation of shaft fracture of EPX vacuum pump
Zkoumání lomu hřídele EPX vakuové pumpy

The thesis language: English

Description:

1. Introduction
2. Theoretical part: a) EPX pump introduction and principle of operation; b) Problem description; c) Description of a critical spot; d) Influence on production.
3. Experimental part: a) Shaft material investigation; b) Tensile stress calculation at the critical spot.
4. Discussion on findings
5. Conclusions

References:

[1] CALLISTER, W. D. *Fundamentals of Materials Science and Engineering*. 7. vyd. New York: John Wiley & Sons, 2007, 722 p. ISBN 0-471-73696-1.
[2] OHRING, M. *Engineering Materials Science*. San Diego: Academic Press, 1995, 827 p. ISBN 0-12-524995-0.
[3] CAMPBELL, F. C.: *Elements of Metalurgy and Engineering Alloys*. Materials Park Ohio: ASM International, 2008, 656 p. ISBN 978-0-87170-867-0.
[4] *ASM Handbook, Volume 11, Failure analysis and Prevention*. Materials Park Ohio: ASM International, 2002. ISBN 0-87170-704-7.

Extent and terms of a thesis are specified in directions for its elaboration that are opened to the public on the web sites of the faculty.

Supervisor: **prof. Dr. Ing. Jaroslav Sojka**

Date of issue: 30.11.2015
Date of submission: 20.05.2016

VYSOKÁ ŠKOLA BÁŇSKÁ - TECHNICKÁ UNIVERZITA
Fakulta metalurgie a mat. inženýrství
OSTRAVA

prof. Ing. Vlastimil Vodárek, CSc.
Head of Department

prof. Ing. Jana Dobrovská, CSc.
Dean of Faculty

Zásady pro vypracování bakalářské práce

I.

Bakalářskou prací (dále jen BP) se ověřují vědomosti a dovednosti, které student získal během studia, a jeho schopnosti využívat je při řešení teoretických i praktických problémů.

II.

Uspořádání bakalářské práce:

1. Titulní list
2. Originál zadání BP
3. Zásady pro vypracování BP
4. Prohlášení + místopřísežné prohlášení
5. Abstrakt + klíčová slova česky a anglicky
6. Obsah BP
7. Textová část BP
8. Seznam použité literatury
9. Přílohy

ad 1) Titulní list je koncipován podle požadavků příslušné oborové katedry.

ad 2) Originál zadání BP obdrží student na oborové katedře.

ad 3) Tyto „Zásady pro vypracování bakalářské práce" následují za originálem zadání BP. („Zásady pro vypracování bakalářské práce" jsou ke stažení na webových stránkách fakulty).

ad 4) Prohlášení + místopřísežné prohlášení napsané na zvláštním listu (ke stažení na webových stránkách fakulty) a vlastnoručně podepsané studentem s uvedením data odevzdání BP. V případě, že BP vychází ze spolupráce s jinými právnickými a fyzickými osobami a obsahuje citlivé údaje, je na zvláštním listě vloženo prohlášení spolupracující právnické nebo fyzické osoby o souhlasu se zveřejněním BP.

ad 5) Abstrakt a klíčová slova jsou uvedena na zvláštním listu česky a anglicky v rozsahu max. 1 strany pro obě jazykové verze.

ad 6) Obsah BP se uvádí na zvláštním listu. Zahrnuje názvy všech číslovaných kapitol, podkapitol a statí textové části BP, odkaz na seznam příloh a seznam použité literatury, s uvedením příslušné stránky. Předpokládá se desetinné číslování.

ad 7) Textová část BP obvykle zahrnuje:

- Úvod, obsahující charakteristiku řešeného problému a cíle jeho řešení v souladu se zadáním BP;
- Vlastní rozpracování BP (včetně obrázků, tabulek, výpočtů) s dílčími závěry, vhodně členěné do kapitol a podkapitol podle povahy problému;
- Závěr, obsahující celkové hodnocení výsledků BP z hlediska stanoveného zadání.

BP nemusí obsahovat experimentální (aplikační) část.

BP bude zpracována v rozsahu min. 25 stran (včetně obsahu a seznamu použité literatury). V případě, kdy zadání BP vychází ze spolupráce se subjekty mimo VŠB -TU Ostrava a řešení studenta, týkající se citlivých dat spolupracujícího subjektu, je zpracováno v samostatné zprávě, tak zveřejněná část BP bude zpracována v rozsahu min. 15 stran a celkový rozsah BP bude min. 25 stran.

Text musí být napsán vhodným textovým editorem počítače po jedné straně bílého neleskleho papíru formátu A4 při respektování následující doporučené úpravy - písmo Times New Roman 12b; řádkování 1,5; okraje – horní, dolní – 2,5 cm, levý – 3 cm, pravý 2 cm, zarovnání do bloku.

Fotografie, schémata, obrázky, tabulky musí být očíslovány a musí na ně být v textu poukázáno. Budou zařazeny průběžně v textu, pouze je-li to nezbytně nutné, jako přílohy (viz ad 9). Odborná terminologie práce musí odpovídat platným normám. Všechny výpočty musí být přehledně uspořádány tak, aby každý odborník byl schopen přezkoušet jejich správnost. Matematické vzorce musí být číslovány (v kulatých závorkách). U vzorců, údajů a hodnot převzatých z odborné literatury nebo z praxe musí být uveden jejich pramen - u literatury citován číselným odkazem (v hranatých závorkách) na seznam použité literatury
Nedostatky ve způsobu vyjadřování, nedostatky gramatické, neopravené chyby v textu mohou snížit klasifikaci práce.

ad 8) BP bude obsahovat alespoň 10 literárních odkazů, z toho nejméně 3 v některém ze světových jazyků. Seznam použité literatury se píše na zvláštním listě. Citaci literatury je nutno uvádět důsledně v souladu s ČSN ISO 690. Na práce uvedené v seznamu použité literatury musí být uveden odkaz v textu BP.

ad 9) Přílohy budou obsahovat jen ty části (speciální výpočty, zdrojové texty programů aj.), které nelze vhodně včlenit do vlastní textové části, např. z důvodu ztráty srozumitelnosti.

III.

Bakalářskou práci student odevzdá ve dvou knihařsky svázaných vyhotoveních, pokud katedra garantující studijní obor neurčí jiný počet. Vnější desky budou označeny takto:

nahoře: *Vysoká škola báňská - Technická univerzita Ostrava*
Fakulta metalurgie a materiálového inženýrství
Katedra . . . . . .

uprostřed: *BAKALÁŘSKÁ PRÁCE*

dole: *Rok* *Jméno a příjmení*

Kromě těchto dvou knihařsky svázaných výtisků odevzdá student kompletní práci také v elektronické formě do IS EDISON. Práce vložená v elektronické formě do IS EDISON se musí zcela shodovat s prací odevzdanou v tištěné formě. Po vložení BP do IS EDISON bude provedena její kontrola na plagiátorství.

IV.

Nesplnění výše uvedených zásad pro vypracování bakalářské práce může být důvodem nepřijetí práce k obhajobě. O nepřijetí práce k obhajobě rozhoduje v tomto případě garant příslušného studijního oboru. Tyto zásady jsou závazné pro studenty všech studijních programů a forem bakalářského studia Fakulty metalurgie a materiálového inženýrství Vysoké školy báňské – Technické univerzity Ostrava od akademického roku 2015/2016.

Ostrava 2. 11. 2015

Prof. Ing. Jana Dobrovská, CSc.
děkanka Fakulty metalurgie a materiálového inženýrství
VŠB-TU Ostrava

P R O H L Á Š E N Í

Prohlašuji, že

- ☐ jsem byl(a) seznámen(a) s tím, že na moji bakalářskou práci se plně vztahuje zákon č. 121/2000 Sb. – autorský zákon, zejména §35 – užití díla v rámci občanských a náboženských obřadů, v rámci školních představení a užití díla školního (§60 – školní dílo);

- ☐ beru na vědomí, že Vysoká škola báňská – Technická univerzita Ostrava (dále jen VŠB – TUO) má právo nevýdělečně ke své vnitřní potřebě bakalářskou práci užít (§35 odst. 3);

- ☐ souhlasím s tím, že bakalářská práce bude archivována v elektronické formě v databázi Ústřední knihovny VŠB – TUO a jeden výtisk bude uložen u vedoucího bakalářské práce. Souhlasím s tím, že údaje o bakalářské práci budou zveřejněny v informačním systému VŠB-TUO;

- ☐ bylo sjednáno, že s VŠB – TUO, v případě zájmu z její strany, uzavřu licenční smlouvu s oprávněním užít dílo v rozsahu §12 odst. 4 autorského zákona;

- ☐ bylo sjednáno, že užít své dílo – bakalářskou práci nebo poskytnout licenci k jejímu využití mohu jen se souhlasem VŠB – TUO, která je oprávněna v takovém případě ode mne požadovat přiměřený příspěvek na úhradu nákladů, které byly VŠB – TUO na vytvoření díla vynaloženy (až do jejich skutečné výše);

- ☐ beru na vědomí, že odevzdáním své bakalářské práce souhlasím s jejím zveřejněním podle zákona č. 111/1998Sb., o vysokých školách a o změně a doplnění dalších zákonů (Zákon o vysokých školách) bez ohledu na výsledek její obhajoby.

Místopřísežně prohlašuji, že jsem celou bakalářskou práci vypracoval(a) samostatně.

V Ostravě 18.5.2016 .....

Pek Bílek
.....
podpis (jméno a příjmení studenta)

ABSTRACT

This Bachelor thesis deals with the problem of occasional shaft thread fracture of EPX vacuum pump. The theoretical part briefly introduces EPX vacuum pump and its operation principle, describes the problem and the critical place and outlines possible causes of failure. The experimental part deals with the investigation of possible causes and is focused mainly with assembly method, shaft design and workmanship, tooling and material properties. The investigation identified a few critical features in shaft design, manufacturing and usage which should be corrected to improve the shaft thread strength.

KEYWORDS

Vacuum pump, shaft thread fracture, 817M40, segregation, undercut, torque

ABSTRAKT

Tato bakalářská práce se zabývá problémem občasného zlomení závitu hřídele vakuové pumpy EPX. Teoretická část stručně představuje EPX vakuovou pumpu a princip jejího fungování, popisuje problém a kritické místo a nastiňuje možné příčiny problému. Experimentální část se pak zabývá vyšetřováním možných příčin a je zaměřena zejména na metody montáže, návrh hřídele a její zpracování, nástroje a vlastnosti materiálu. Vyšetřování odhalilo několik kritických míst jak v návrhu, tak výrobě a použití hřídele, které by měly být odstraněny, aby se zvýšila pevnost závitu hřídele.

KLÍČOVÁ SLOVA

Vakuová pumpa, lom závitu hřídele, 817M40, segregace, zápich, utahovací moment

I would like to thank to my supervisor prof. Dr. ing. Jaroslav Sojka for his willingness, help and valuable recommendations provided during the work on the thesis.

I wish also to thank to my colleague ing. Tomáš Horák for his suggestions provided during the evaluation of the shaft design.

Finally, I do want to thank to my wife Renata for here support and patience during my study.

Table of contents

1 Introduction 3

2 Principle objectives of the Bachelors thesis 4

3 An introduction to EPX pump 5

3.1 A brief history of EDWARDS 5

3.2 EPX dry vacuum pump 6

3.2.1 Holweck drag stage 8

3.2.2 Regenerative stage 9

3.2.3 Performance 10

3.3 Rotor-shaft connection 12

3.3.1 Rotor related forces during pump operation 12

3.3.2 Rotor – shaft fixing interface arrangement 12

4 Problem definition – Shaft fracture 15

4.1 Problem description 15

4.2 Possible causes for shaft fracture 16

4.2.1 Assembly method 17

4.2.2 Tooling 18

4.2.3 Shaft design and workmanship 18

4.2.4 Shaft material 22

5 Investigations and findings 25

5.1 Assembly method 25

5.1.1 Assembly procedure 25

5.1.2 Assembly procedure not understood 25

5.1.3 Operator 25

5.2 Tooling 26

5.3 The shaft thread and neck design 26

5.3.1 Calculation of the preload force 26

5.3.2 Design of the shaft thread 27

5.3.3 Design of the neck 28

5.4 Shaft samples investigated 28
5.4.1 Thread dimensions 29
5.4.2 Undercut shape 30
5.4.3 Cracks in material due to incorrect manufacturing 31
5.4.4 Shaft material investigation 33
6 Summary and discussion 37
6.1 Summary 37
6.2 Conclusion and recommendations 38
7 Experimental 39
8 References 40

1 Introduction

Vacuum pumps belong to a group of very sophisticated machines where requirements for performance, reliability and lifetime are pushed to the limits to withstand broad application conditions of many customers.

Within the effort to fulfill these requirements a broad portfolio of vacuum generating principles was developed. Various vacuum equipment producers like Varian, Leybold, Edwards, Pfeifer, Iwata, Vacuubrand and others produce pumps which are different in appearance and technical details however they share the same basic principles.

Edwards developed a pump which is being produced solely by this company and has currently no competitive counterpart produced by any other provider. The pump is called EPX. This pump combines well known vacuum generating methods in a new fashion to simplify both its assembly and operation. The pump utilizes single shaft design where all main parts are mounted on a central shaft going through the pump. Such mechanical arrangement is somewhat more demanding on quality of assembly parts and the assembly process itself. In case one of main quality conditions is compromised this can lead to various problems both in assembly and operation.

One of the problems which occasionally occur during assembly process of EPX pump is fracture of the shaft in its narrowest place – top shaft thread neck. The thread and related parts are responsible for fixing vacuum generating rotor which is attached to the shaft. Shaft fractures generate unwanted production delays and extra cost involved in manpower and spare parts required for rework.

2 Principle objectives of the Bachelors thesis

In order to minimize the losses mentioned in Chapter 1 there was an investigation conducted to identify potential causes for such fracture.

The main objective of the Bachelors thesis is to summarize the investigation. This covers a list of possible causes for shaft thread fracture, investigation of available fractured shaft samples and discussion over results.

The thesis is divided into a few chapters:

The theoretical part (Chapters 3 and 4) introduces briefly Edwards Company and EPX pump and also outlines the principle of its operation. Then describes the place of interest and critical spot where fracture occurs. Finally the part deals with possible causes which can induce shaft fracture and gives brief rational behind each of them.

The practical part (Chapter 5) contains experimental results and collected findings for possible causes outlined in Chapter 4.

Chapter 6 interprets and discusses the results found and outlines the causes of the problem.

3 An introduction to EPX pump

3.1 A brief history of EDWARDS

Edwards has come a long way since its foundation in 1919 when physicist F.D. Edwards began importing vacuum equipment and established an equipment and service business from his office in South London, England. Today the company specializes in designing and production of vacuum equipment and abatement systems for usage in both scientific and industrial sectors.

The company operations are spread in more than 30 countries worldwide now with more than 4200 employees and +1 billion USD revenues.

In 2014 the company was acquired by a Swedish producer of compressor technique – Atlas Copco – to create its new Vacuum solutions division.

Edwards is especially recognized for the following products [1]:

	GXS DRY PUMP Highly intelligent GXS range of pumps provides robust and reliable operation even in harsh industrial applications. Minimal maintenance is required and low utilities and energy usage costs mean substantial savings.		CXS DRY PUMP Providing exceptional performance even in harsh chemical and pharmaceutical processes, the CXS range combines high reliability with a low cost of ownership.
	iXL DRY PUMP iXL120 and iXL1000 are compact, low energy, dry pumps (110-930 m^3/h) for wafer handling and other clean duty applications. They provide fast pump down of load lock chambers with extremely low energy consumption.		eZENITH Integrated vacuum pumping and abatement in a single system to provide semiconductor manufacturers with a highly efficient, low cost of ownership solution that meets the latest manufacturing and environmental requirements.
	nXDS DRY PUMP The intelligent control functions and up to five year service interval offer low cost of ownership, making it the small dry pump of choice for today's most advanced technologies. Pump range includes 6, 10, 15 and 20 m^3/h.		nEXT TURBO Designed to combine all the latest technological advances in turbomolecular pumps with end-user serviceability, delivering a truly class leading product. Pump sizes available offering true 240, 300 and 400 liters per second pumping speed performance.

	STP TURBO The ideal choice for critical and demanding applications, providing exceptional performance, reliability and maintenance free pumping. The multi-axis magnetic bearing system ensures there is no risk of contamination, while minimizing noise and vibration with a reliable, consistent performance.		GAMMA VACUUM Titan™ Ion Pumps Part of the Gamma Vacuum product range. Ion pumps are used in a wide variety of high and ultra-high vacuum (UHV) environments.

3.2 EPX dry vacuum pump

The EPX pump and its predecessor IPX deserve to be added to the group above as they combine known vacuum generating principles which put together in a smart arrangement create a unique pump. No competitor is currently able to offer an alternative to this pump in terms of form and performance thus making this product unique among all competition in vacuum business to date.

The IPX pump was first offered to customers in 1998 and in 2002 the result of its evolution – EPX – was launched (Figure 1).

Figure 1: EPX Pump and its relative size [1]

The EPX Series offers on-tool pumping in a very light small package and delivering exceptionally clean vacuum. Using a unique, patented, single-shaft regenerative Holweck® stage mechanism, EPX pumps are capable of evacuating from atmosphere to ultra-high vacuum (UHV) level base pressure (10^{-6} mbar) and can operate continuously at all inlet pressures as the pump can be aerated at full speed with no harm to it (contrary to Turbomolecular pumps).

The EPX pump series supports clean and light duty semiconductor processing applications such as ash/strip and implant end station applications.

Typical applications include:

- Load lock
- Metrology
- Transfer Chambers
- Ashing/Striping
- PVD

The main motivation behind the development of the EPX series of dry (=no fluid in vacuum space) pumps was to create a pump capable of reaching high vacuum, with significant pumping speed and itself exhausting to atmospheric pressure. Typically high vacuum (and beyond) is achieved in two (or more) pumping 'stages': primary (10^3 to $10^{-2}/10^{-3}$ mbar) and secondary pumps to (and beyond) high and ultra-high vacuum levels $<10^{-10}$ mbar. As a single high vacuum mechanism the EPX would thus simplify system complexity and minimize costs, services, maintenance and footprint.

EPX pumps achieve performance by means of a combination of molecular drag and fluid dynamic mechanisms. They consist of inlet molecular drag stages of the Holweck type [2] with an "in-series" multistage regenerative compressor as the backing stage, both of which are mounted on the same shaft.

The simplified pump configuration is illustrated in Figure 2:

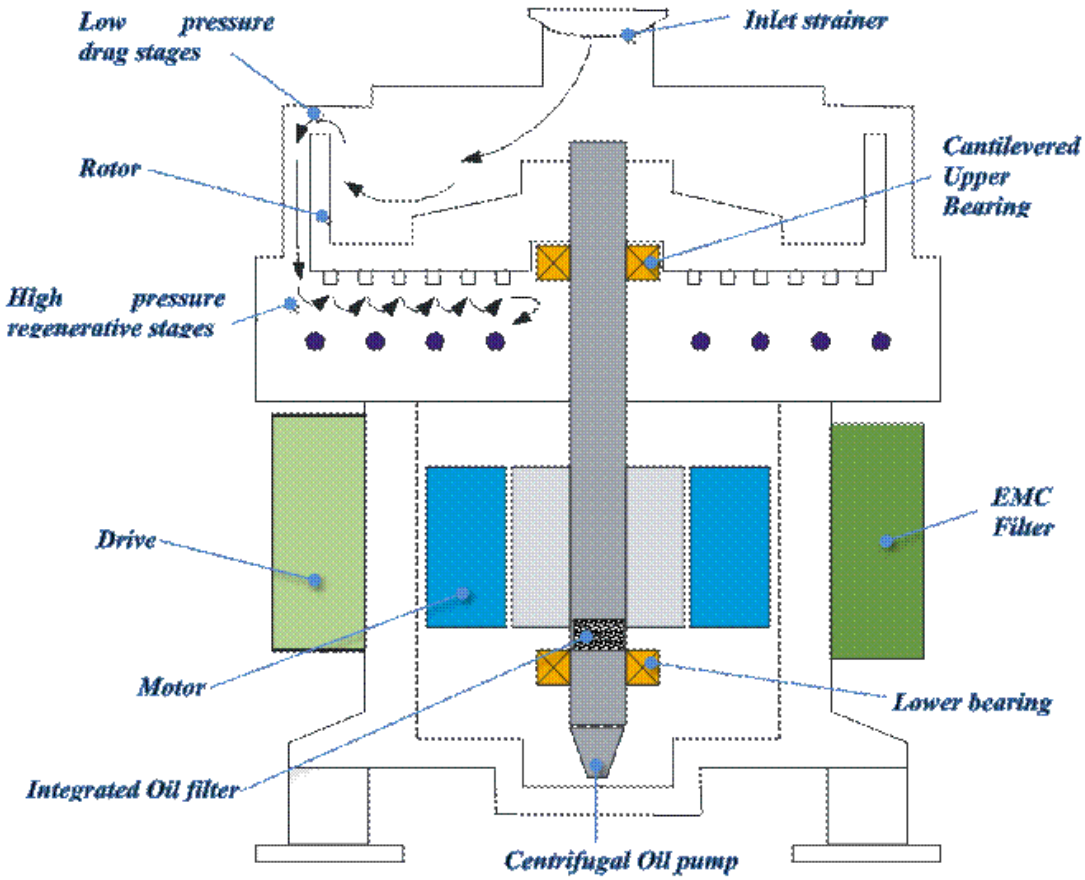

Figure 2: Simplified cross section of EPX pump [3]

Both main mechanisms are placed on a rotor which rotates at a high speed. Gas flows from inlet through low pressure drag stages, then beneath the rotor to high pressure regenerative stages and finally to exhaust at atmospheric pressure. Rotor is placed on a single shaft and held using 2 bearings construction. Oil is distributed to both bearings from an oil reservoir using centrifugal pump.

3.2.1 Holweck drag stage

The Holweck stage (Figure 3) comprises a stator in which are machined a set of parallel helical grooves forming a set of parallel pumping channels (Figure 4).

Figure 3: Holweck stage

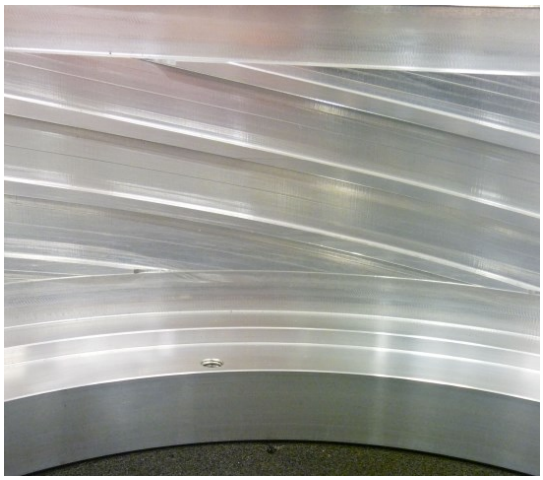

Figure 4: Helical grooves of Holweck stage

The rotor is simply a plane cylinder. A particular feature is that the helical grooves occupy less than one turn so that the pressure distribution is the same in each channel. Since there are no relatively high pressure sections adjacent to lower pressure sections, leakage between channels is minimized and the mechanism is relatively efficient both in terms of compression ratio achievable per unit length of channel and in terms of pumping speed. This design feature enables the development of an axially compact machine but its limitation on compression ratio does lie in the fact that the pumping channels are relatively short so that, for the same peripheral speed, the compression ratios achievable are less than those for a multiturn helix.

The compression ratios are maximized by effectively isolating the higher pressure sections. This also minimizes back leakage and keeps speed efficiency high. Additionally this means that, for practical dimensions and rotational frequencies, the exhaust pressure cannot be more than a few mbar. Even so, useful compression ratios can be achieved for rotational frequencies of 300 Hz and the machine can develop an exhaust pressure that is sufficiently high for the fluid dynamic or regenerative compressor stage to operate.

A simple theory of the Holweck stage can be developed along similar lines to that described by Helmer [4]. Gas transport is described by the Knudsen transitional flow expression (Equation 1):

$$\frac{\mu A}{L} = \left\{C_m + C_v\left(\frac{1+k_1P}{1+k_2P}\right)\right\}\frac{1}{P}\frac{dP}{dx}$$

Equation 1: Knudsen transitional flow expression

where:

k_1, k_2 - the constants in the Knudsen transitional flow formula

C_m - the molecular channel conductance [m^3s^{-1}]

C_v - the viscous laminar channel conductance (at pressure P [Pa] and linear distance x [m])

μ is the component of peripheral velocity [ms^{-1}] (~150 m/s at 300 Hz).

A is the cross-sectional area [m^2]

L the total length of a channel [m]

This solves to yield Equation 2:

$$K \sim e^{\left(\frac{\mu L}{d}\right)}$$

Equation 2: Knudsen formula solved

where:

K - the compression ratio channel exhaust to inlet

d - the depth of the channel [m].

Equations 1 and 2 show that compression ratio is very sensitive to the channel area which falls dramatically as the channel area is increased.

The inlet stage of EPX machine is primarily designed for volumetric capacity and modest compression ratio; the depth of the channels is significant. Later stages are designed with relatively shallow channels in order to maximize compression ratio so the Holweck stages near the exhaust have channels of relatively small depth.

3.2.2 Regenerative stage

The regenerative stage of the pump, sometimes called a vortex or fluid dynamic pump is illustrated in Figure 5.

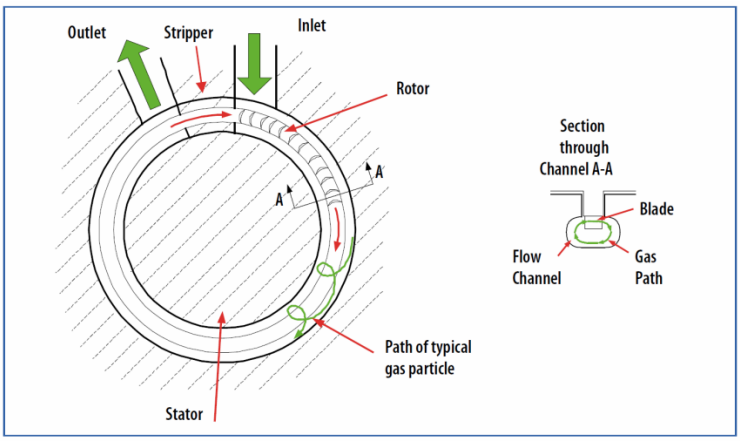

Figure 5: Vortex pump principle scheme [5]

The rotor comprises a disk on which a set of axially oriented vanes are circumferentially arranged (Figure 6). As the disk spins, the vanes move at high speed through a toroidal channel stator (Figure 7).

Figure 6: Oriented vanes on rotor

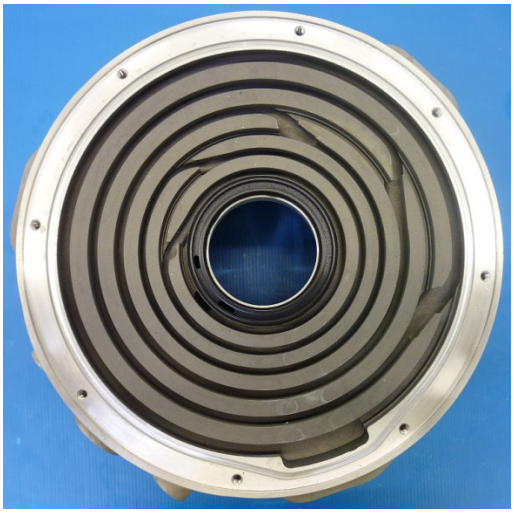

Figure 7: Toroidal channels in stator

Through most of its length the toroidal channel cross section is circular and significantly larger than the vanes. The inlet and outlet ports are separated by a portion of the channel, referred to as the "stripper," see Figure 5. Here the channel cross section changes to a shape similar to and slightly larger than the vane cross section.

The motion of the vanes entrains, and induces a rotation in, the gas so that the gas follows a helical path though the toroidal stator, passing through the rotor vanes and re-entering them several times during one rotation as in Figure 5.

The circumferential rotation of the gas is thus regenerated a number of times during each rotation—hence the reference to the device as a regenerative compressor.

3.2.3 Performance

EPX pump exists in two major configurations - EPX 180 and EPX 500. Performance comparison of the two is summarized in Table 1:

Pump type	EPX 180	EPX 500
Peak speed	180 m^3h^{-1} (50 ls^{-1}) at 2.10^{-1} mbar	500 m^3h^{-1} (140 ls^{-1}) at 2.10^{-4} mbar
Ultimate vacuum	<1 x 10^{-4} mbar	<1 x 10^{-6} mbar
Compression ratio	>1 x 10^7	>1 x 10^9
Noise	<59 dB(A)	<59 dB(A)
Power at ultimate	1.4 kW	1.6 kW
Weight	45.2 kg	45.4 kg

Table 1: Main performance parameters of EPX pump versions [6]

The main difference between the two is a change in drag stage arrangement. EPX 500 is equipped with helical rotor (Figure 8) which serves as a booster and is responsible for high pumping speeds. Its grooves are very deep and short which causes big volumes of gas are pumped during operation.

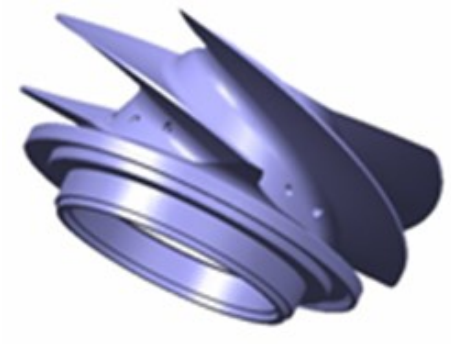

Figure 8: Helical rotor

Holweck stage features a longer path thus increasing compression ratio. Cross sections of both versions are shown in Figure 9. Regenerative stages remain the same.

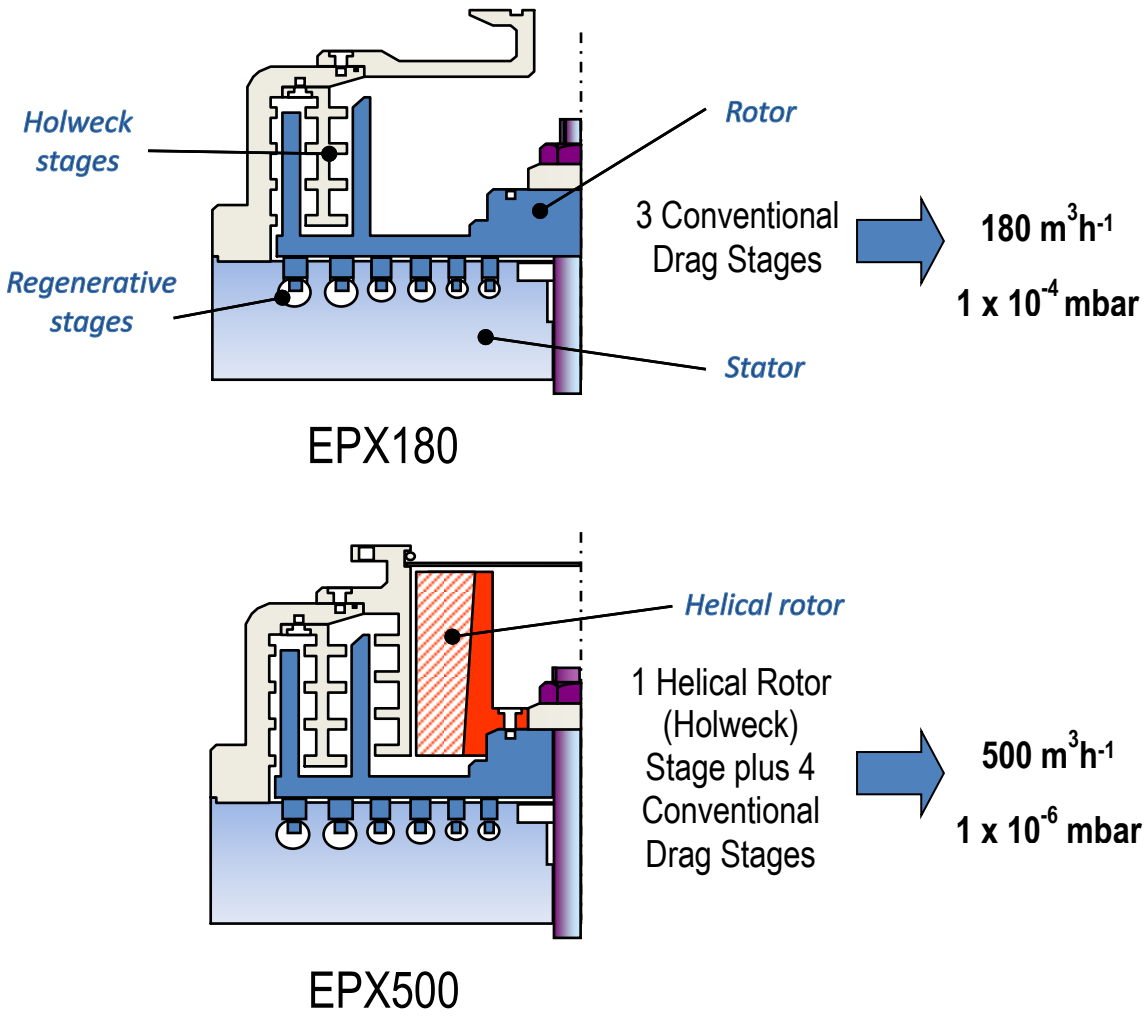

Figure 9: EPX 180 and EPX 500 pumping mechanisms cross sections [1]

3.3 Rotor-shaft connection

The chapter explains the rotor-shaft interface and its arrangement and describes the critical place.

As it was described in previous chapters vacuum in EPX pump is generated by rotation of rotor which is fixed on a shaft in appropriately arranged stator. The rotation speed of rotor is very high and in standard operation mode the frequency of rotation up to 300 Hz is reached which means linear speed 150 $m.s^{-1}$.

Due to the weight of rotor-shaft assembly and high rotation speed the kinetic energy accumulated in rotating parts is very high and can be compared with kinetic energy of 1100 kg heavy car going at 40 $km.h^{-1}$ speed.

3.3.1 Rotor related forces during pump operation

Not only kinetic energy but also appropriate axial and radial forces from rotor create extra demand on the shaft and stiffness of the whole pump body. Radial forces are well controlled by means of balancing and are on relatively low level unless external unbalance is introduced during pump lifetime. Contrary to that axial forces can dynamically change during different pump operation modes.

During operation, rotor interfaces with low pressure area (above rotor) and high pressure area with pressure up to atmospheric in regeneration area (bellow rotor) (Figure 10). Such pressure difference generates a lifting force which is constantly pushing the rotor upwards during operation. Simplified calculation assuming zero pressure above rotor and about 30 % of atmospheric pressure in average bellow rotor suggests the lifting force can reach easily 1500 N.

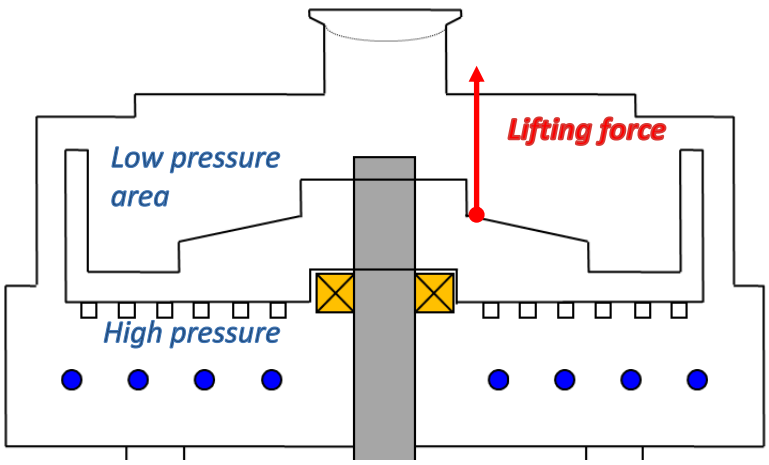

Figure 10: The pressure difference is generating a lifting force [1]

3.3.2 Rotor – shaft fixing interface arrangement

The pump rotor is fixed to the shaft during pump assembly and stays at the same position during pump lifetime unless service operation which requires rotor removal is

performed. The whole assembly consists of 3 additional parts besides shaft and rotor – spring guide, Belleville washer and a nut.

The mechanical arrangement of the interface is shown in Figure 11:

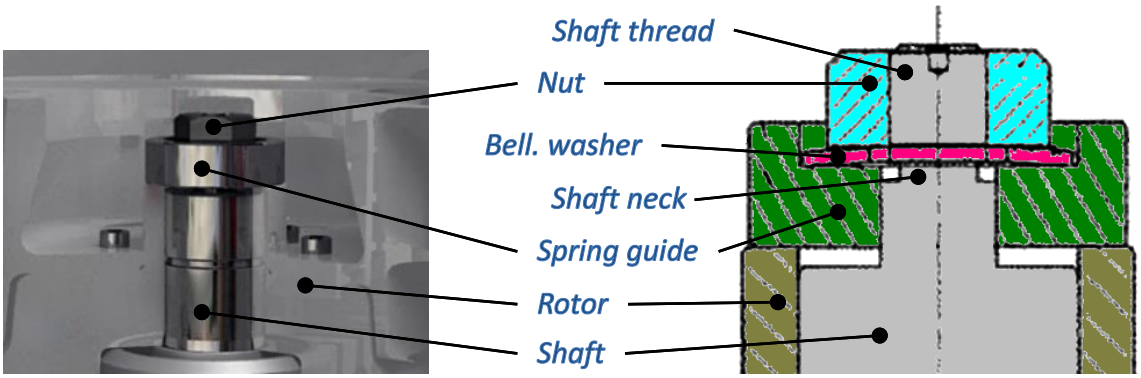

Figure 11: Cross section of rotor-stator interface [1]

3.3.2.1 Spring guide

It is a machined metal part of circular shape with part of the surface sandblasted (Figure 12). Its main function is to hold rotor in place against axial forces. It also serves as a support for Belleville washer.

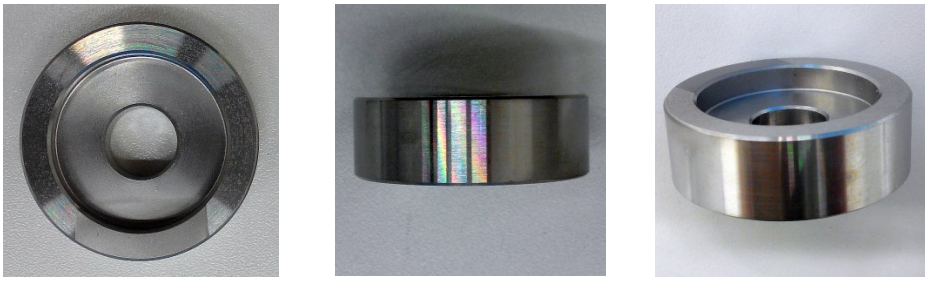

Figure 12: Spring guide

3.3.2.2 Belleville washer

Belleville washer (Figure 13) is a conical washer used for maintaining a uniform tension load on a bolt. If it is not completely flattened out, it serves as a spring in the bolt joint. It creates preload which is applied to the nut and prevents the nut from being loosen during pump operation – this could cause unwanted mutual rotor-shaft rotations and in the worst case the rotor to become loose.

Figure 13: Belleville washer

3.3.2.3 The nut

The nut sits on top of the shaft where M10 thread is placed. It holds the Belleville washer and creates the preload due to torque applied during assembly (45 N.m). The nut has a left-handed thread due to clockwise rotor rotation (Figure 14).

Figure 14: The nut

3.3.2.4 The shaft

Main shaft of the EPX pump is a centerpiece of the whole pump assembly. It features a sophisticated shape and each part of the shaft has its own function (Figure 15).

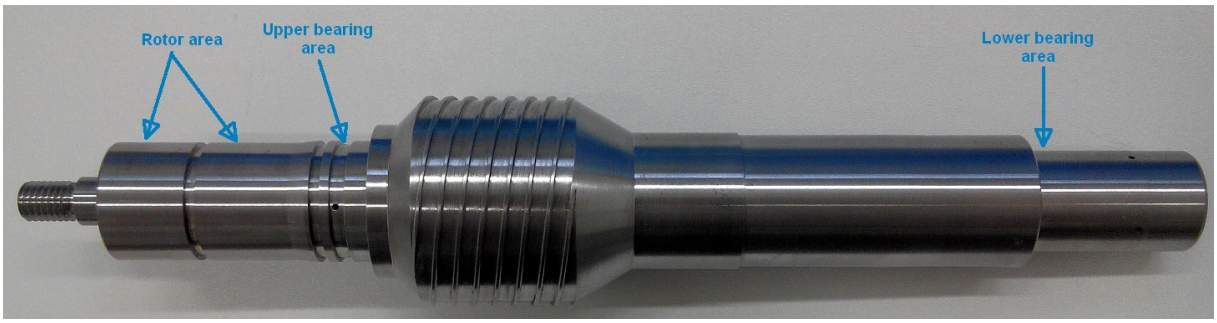

Figure 15: The EPX shaft

The shaft is made from 817M40 BS970-3:1991 (EN24T) alloy steel which comes to shaft supplier in properly sized round bars made by continuous casting method.

4 Problem definition – Shaft fracture

The following chapter contains introduction to the problem and a list of possible causes with reasoning for each cause.

4.1 Problem description

When EPX pump is being assembled the rotor is put on the shaft for the first time at one part of the process, then spring guide and spring washer is added and the whole assembly is secured with a nut (Figure 16). The torque used for nut tightening is 45 N.m.

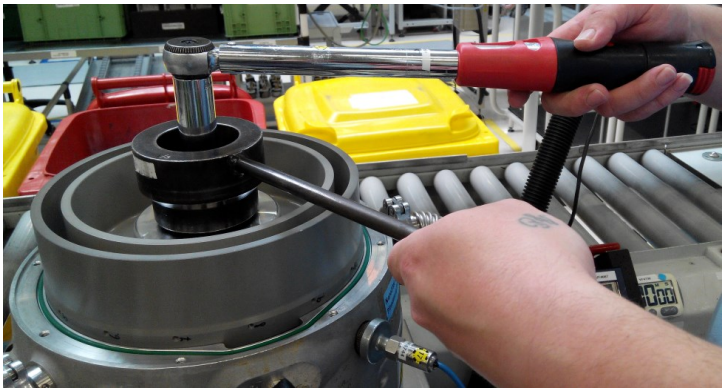

Figure 16: Rotor being attached to the shaft - nut tightening

Occasionally a fracture of the shaft thread occurs during this step. This fault results in with thread and nut separated from the rest of the shaft (Figure 17).

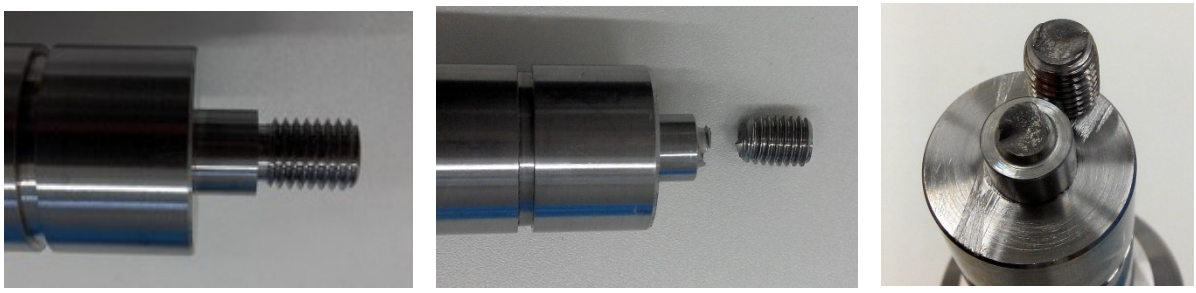

Figure 17: Examples of good and fractured shaft (other parts removed)

The fault occurs randomly, sometime in waves, which means it can be experienced a few times a week during its peek occurrence and then it does not appear for months. There are a few features of this fault which always occur when this fracture happens:

1) The shaft always cracks in the narrowest spot of it which means the undercut between the thread and the rest of the shaft.
2) Although rotor is usually removed from shaft repeatedly during assembly so the nut tightening occurs a few times before rotor is finally attached to the shaft the crack always occurs during the first nut tightening step. It was NEVER experienced in later stages.
3) This fault has NEVER been experienced in later stages of the assembly process nor during long term pump operation.

The reject rate for this failure in 2015 was ~ 0.3 %.

If the thread fracture occurs it renders the shaft to be unusable and results in rework when pump needs to be disassembled and shaft to be exchanged. This procedure is costly in terms of time, manpower and spares to be used.

4.2 Possible causes for shaft fracture

When investigating any issue it is necessary to summarize possible causes for the problem. One of quality tools which can be used for this purpose is called Cause & Effect Diagram (CED) [7].

The CED was developed by Kaoru Ishikawa, who pioneered quality management processes in the Kawasaki shipyards, and in the process became one of the founding fathers of modern management. It belongs to so called Seven basic tools of quality [8]. The CED is used to explore all the potential or real causes (or inputs) that result in a single effect (or output). Causes are arranged according to their level of importance or detail, resulting in a depiction of relationships and hierarchy of events. This can help to search for root causes, identify areas where there problems may be, and compare the relative importance of different causes.

The CED is also known as the fishbone diagram because it was drawn to resemble the skeleton of a fish, with the main categories drawn as "bones" attached to the spine of the fish.

Causes in CED are frequently arranged into six major categories known as 6M (man, methods, materials, machinery, management and measurement). However this is not a rule and categories can be named freely to better describe the specific problem being solved.

One of possible evolutions how to construct CED diagram for the problem described in this thesis is shown in Figure 18:

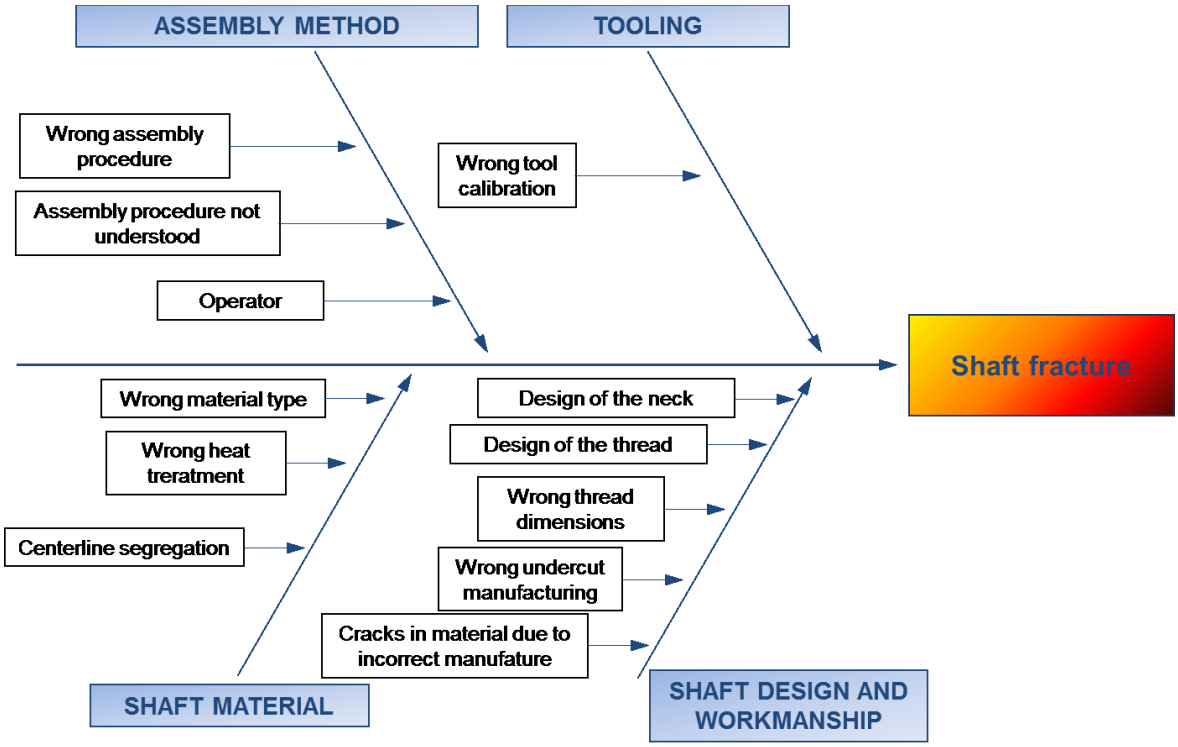

Figure 18: Cause & Effect diagram for EPX shaft fracture

For this specific problem main categories were named as follows: Assembly method, Tooling, Shaft material and Shaft design and Workmanship.

The amount of possible causes in general is usually very high so the prioritization should be done utilizing scoring each cause by a group of experienced people and choosing highest ranked causes to be investigated first.

Number of causes in the CED constructed for this thesis contains a relatively small number of issues thus all of them can be discussed and investigated within the scope of this thesis without prioritization.

The following chapters discuss each cause and possible failure mode which to be investigated later in the thesis.

4.2.1 Assembly method

Assembly method category contains possible causes related to assembly procedure documentation, its interpretation and implementation by operators.

4.2.1.1 Wrong assembly procedure

Assembly procedure (sometimes called "Standard operating procedure") is a basic document describing exact step-by-step sequence of how to assemble parts together during process. Generally it is not infrequent especially during early stages of production startup the procedures are not 100% fool proof mainly due to the lack of experience with the product and thus assembly procedures may require improvements during the product lifetime either to improve correctness of the procedure or to upgrade the procedure to implement new technique or measurement required.

Procedure correctness, simplicity and its suitability is to be investigated.

4.2.1.2 Assembly procedure not understood

Despite all the effort done to make assembly procedures as simple and clear as possible misunderstanding of it can sometimes happen and the operators can interpret the procedure in a different way than it is intended. The deviation may not be visible on a first sight but can cause significant problems either during assembly, testing or product lifetime.

Understanding of current assembly instructions and product assembly sequence is to be investigated.

4.2.1.3 Operator

Operators in general introduce a variation to the process. This source of variation includes the operator's physical and emotional status and level of skill, physical fitness, health problems, emotional stability etc. An operator's lack of understanding equipment and material variations due to lack of training belongs also to this category.

Occurrence of the problem per operator is to be investigated.

4.2.2 Tooling

Tooling used to connect rotor with shaft of EPX pump is quite simple as only tightening of the nut by standard torque wrench is used. This torque wrench is set to 45 N.m and regularly externally calibrated once a year. This period was set based on general experience with this type of tooling.

Calibration validity and actual torque value set is to be investigated.

4.2.3 Shaft design and workmanship

The following chapter deals with the shaft design and quality of its manufacturing. The main interest is put to the design and manufacturing of its critical place (undercut, “the neck”).

The excerpt of critical place from shaft drawing and actual photo of the place is shown in Figure 19:

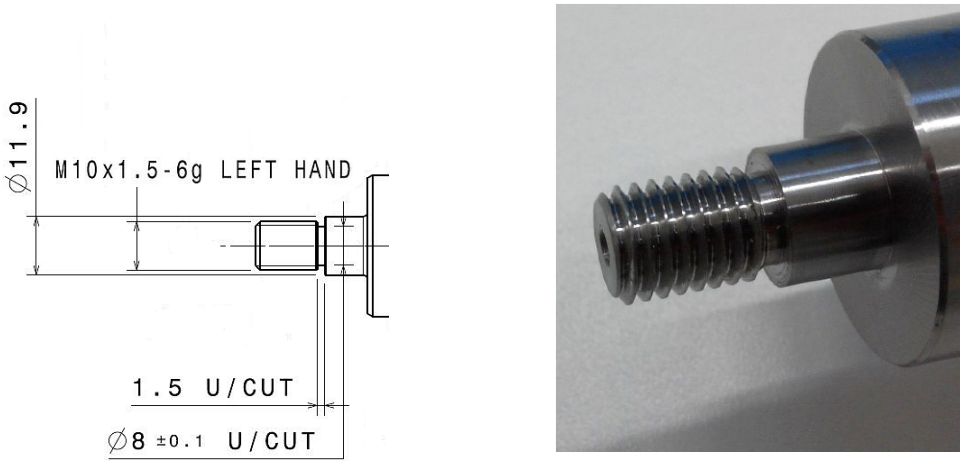

Figure 19: Excerpt from shaft drawing and machined shaft [1]

4.2.3.1 Tensile stress calculation

When a bolt is tightened to clamp the parts together the neck and thread sustain a tensile stress due to being stretched. An adequate clamping (preload) prevents relative motion between parts of the joint. Measuring a bolt's clamp force is difficult, especially under production assembly conditions. The preload generated by a bolt can be indirectly controlled by regulating the applied torque. This method, known as a torque control, is by far the most popular method of controlling a bolt's preload. There is a relationship between the torque applied to a bolt and the resulting preload. The following procedure [9] gives guidance for calculating such stress introduced to the thread and to the neck of the shaft thread (Figure 20). The formulae used are applicable to metric and unified thread forms which have a thread flank angle of 30° (for a basic terminology of thread see Figure 21).

The calculation procedure distinguishes between thread and underhead friction.

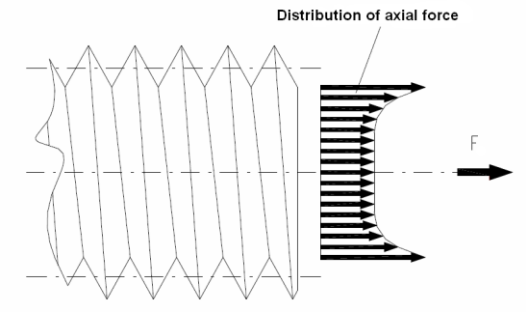

Figure 20: Distribution of axial force [10]

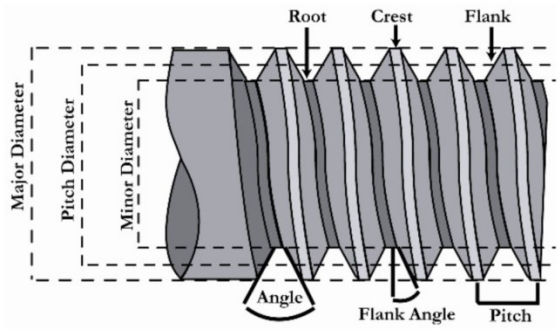

Figure 21: Description of metric thread main dimensions [10]

Axial force ***F*** can be calculated using the following formula (Equation 3):

$$F = \frac{T}{\left[(0.159\,.\,P) + (0{,}577\,.\,d_2\,.\,\mu_T) + \left(D_f\,.\,\frac{\mu_H}{2}\right)\right]}$$

Equation 3: Calculation of axial force by torque given

where:

T	Torque [N.m]
d_2	Pitch diameter of the thread [m]
P	Pitch of the thread [m]
μ_T	Thread friction coefficient
μ_U	Undernut friction coefficient
D_f	Effective frict. diameter of the nut [m]
F	Preload force [N]

The calculated force ***F*** can be then used for calculating tensile stress either in the thread (Equation 4) or in the neck (undercut) (Equation 5) using the following formulae:

$$\sigma_T = \frac{F}{A_T}\left(< \frac{R_e}{k}\right)$$

Equation 4: Tensile stress in thread

$$\sigma_K = \frac{F}{A_N}\left(< \frac{R_e}{k}\right)$$

Equation 5: Tensile stress in neck

where:

A_T	Effective section of the thread [m^2]
A_K	Effective section of the neck [m^2]
σ_T	Tensile stress in thread [MPa]
σ_K	Tensile stress in neck [MPa]
R_e	Yield strength [MPa]

k Safety factor

Effective sections can be calculated using following formulae:

$$A_T = \frac{\pi \,.\, (d_2 + d_3)^2}{16}$$

Equation 6: Effective section of the thread

$$A_K = \frac{\pi \,.\, {d_K}^2}{4}$$

Equation 7: Effective section of the neck

where:

d_3 Minor diameter of the thread [m]

d_K Shaft neck diameter [m]

The maximus stress in the material to be kept bellow yield stress value of selected material divided by chosen safety factor. For R_e=680 MPa and k=1.5 [11] maximum stress allowed in this situation is 453 MPa.

A problem exists in that friction has a large influence on how much torque is converted into preload. Besides the torque required for stretching the bolt, torque is also required to overcome friction in the threads and under the nut face. Typically, only 10 % of the torque is used to stretch the bolt. Of the remaining torque, typically 40 % is dissipated in the threads and 50 % under the nut face [12]. Because friction is such an important factor in the relationship between torque and preload, variations in friction have a significant influence on the bolt's preload. Different bolt surface finishes have different friction values. For example the torque required for a socket headed screw will not be the same as that one required for the same size standard hexagon head bolt. The larger bearing face of the standard hexagon bolt will result in an increased torque being required compared to a socket headed screw. This is because more torque is being dissipated between the nut face and the joint surface.

4.2.3.2 Design of the thread

Screw thread of the EPX shaft must withstand comparable tensile stress as the shaft neck. General rules for screw thread load calculation are described in VDI 2230 directive [9].

The thread used on EPX shaft is a standard ISO M10x1.5-6g thread left-hand.

Calculation of tensile stress in the thread and suitability of the thread size chosen is to be evaluated.

4.2.3.3 Design of the thread neck

Thread neck is a place where fracture of shaft occurs. It is the narrowest place of the whole shaft and the place where the highest load is concentrated when rotor is positioned on the shaft and secured with a nut and a Belleville washer. The tensile stress induced by applied 45 N.m torque must stay under allowed level given by the material used for shaft manufacture and a safety factor used.

Calculation of the tensile stress in the neck is to be calculated and compared with the design of the neck diameter and tolerancing.

4.2.3.4 Wrong thread dimensions

Aside from correct thread dimension design the manufacturing of the thread can change overall strength property of the thread.

Investigation of designed thread with reference thread gage is to be carried out.

4.2.3.5 Wrong undercut manufacturing

An undercut allows threads to be cut on a component up to the end without the end face of the screwing tool fouling the component. Design requirements are usually for a control of the dimensions of the undercut to avoid weakening of the section and to reduce stress concentration. Standard appearance of such undercut is shown in the following picture (Figure 22) [13].

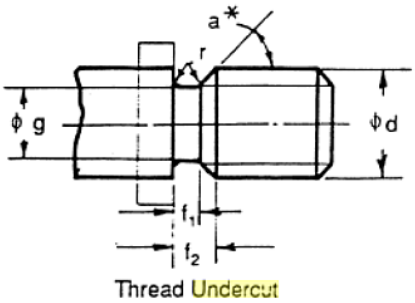

Figure 22: Shape of undercut

In case of EPX shaft the undercut creates “the neck” thus the narrowest point of the shaft. When the undercut is not manufactured correctly or the thread is not ended correctly in the undercut such place can serve as a crack initiator which can cause shaft fracture.

The manufacturing quality and radiuses are to be investigated.

4.2.3.6 Cracks in material due to incorrect manufacture

The manufacturing if done incorrectly with respect to the design or material can introduce unwanted stress to the material which can result in microscopic cracks causing weakening of the material thus decreasing the tensile strength of the material.

Occurrence of cracks in the thread root and undercut are to be investigated.

4.2.4 Shaft material

Once the type of material is selected for parts manufacturing and successfully tested it is important to keep the material properties and quality on the same level throughout the pump manufacturing lifetime. If the material properties deteriorate it can have significant consequences on the material behavior and can lead to unwanted faults or breakdowns.

4.2.4.1 Wrong material type and heat treatment

817M40 (EN24T) [14] steel is readily machineable and combines a good high tensile steel strength with shock resistance, ductility and wear resistance. It is widely used engineering steel with a tensile strength of 850/1000 MPa. It has reasonably good impact properties at low temperatures, although it is also suitable for a variety of elevated temperature applications. 817M40 is most suitable for the manufacture of parts such as heavy-duty axles and shafts, gears, bolts and studs. 817M40 can be further surface-hardened typically to 58-60 HRC by induction or nitride processes, producing components with enhanced wear resistance [15].

Typical heat treatment to "T" condition includes Quenching, Tempering and Stress relieve steps:

1. Hardening:

   Heating uniformly to 820/850 °C until heated thoroughly. Quenched in oil.

2. Tempering:

   Heated uniformly and thoroughly at the selected tempering temperature, up to 660 °C and held at heat for two hours per inch of total thickness. Tempering between 250-375 °C is not recommended as it can seriously reduce the steels impact value.

3. Stress Relieving:

   Heated slowly to 650-670 °C, cooled in a furnace or in air.

Chemical and mechanical properties can be found in Table 2 and Table 3:

817M40 (EN24T) chemical composition	
Carbon	0.36-0.44 %
Silicon	0.10-0.40 %
Manganese	0.45-0.70 %
Sulphur	0.040 % Max
Phosphorus	0.035 % Max
Chromium	1.00-1.40 %
Nickel	1.30-1.70%
Molybdenum	0.20-0.35 %

Table 2: Chemical composition of 817M40 steel

817M40 (EN24T) - mechanical properties		
Max Stress	850-1000 MPa	
Yield Stress	680 MPa Min	(up to 150 mm LRS)
0.2% Proof Stress	665 MPa Min	(up to 150 mm LRS)
Elongation	13 % Min	(9 % if cold drawn)
Impact KCV	50 Joules Min	(up to 150 mm LRS)
Hardness	248-302 Brinnel	(850-1000 MPa)

Table 3: Mechanical properties of 817M40 steel

Selected mechanical properties and metallographic samples to be investigated to check the material was of correct type and its structure is in accordance with prescribed heat treatment.

An investigation of fracture area is to be also carried out to check the type and properties of the fracture and presence of inclusions and other anomalies.

4.2.4.2 Macrosegregation (Centerline segregation) [16]

Macrosegregation refers to variations in composition that occur in metal alloy castings and range in scale from several millimeters to centimeters or even meters. The cause of macrosegregation is relative movement or flow of segregated liquid and solid during solidification. Most alloy elements have a lower solubility in the solid than in the liquid phase, as shown by the partial equilibrium phase diagram in Figure 23. During solidification, the solutes are therefore rejected into the liquid phase, leading to a continual enrichment of the liquid and lower solute concentrations in the primary solid.

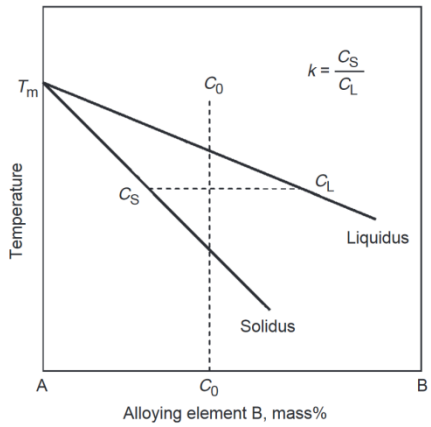

Figure 23: Phase diagram showing different solubility in solid and liquid phases

Due to the solidification direction towards the center of the casting the macrosegregation is concentrated there and causes so called centerline segregation.

A sulfur print showing a typical centerline segregation pattern in a slab is shown in Figure 24:

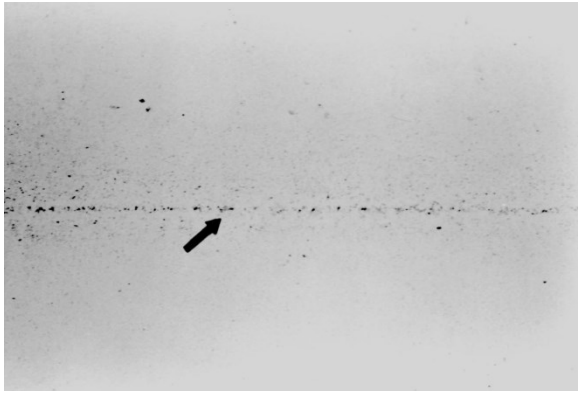

Figure 24: Sulfur print showing centerline segregation (courtesy of IPSCO Inc.)

These compositional variations negatively impact the subsequent processing behavior and properties of cast materials (strength) and can lead to rejection of cast components or processed products. It is present in virtually all casting processes, including continuous, ingot, and shape casting of steel, cast iron, aluminum and copper alloys, casting of single-crystal super alloys, semisolid casting, and growth of semiconductor crystals.

The occurrence of centerline segregation is to be investigated. As the shaft is made from continuously casted slab the shaft neck is positioned in the center of the slab after manufacturing. If the segregation occurs it can deteriorate strength of the shaft neck.

5 Investigations and findings

The following chapter deals with the investigations of the EPX shaft samples described earlier and procedures related to shaft assembly. The structure of investigations follows points defined by Ishikawa diagram (Chapter 4.2).

5.1 Assembly method

This chapter deals with the investigation of assembly related procedures.

5.1.1 Assembly procedure

The assembly procedure was investigated (cannot be shown due to confidentiality) and the following can be concluded:

- the procedure is described in approved operational procedure;
- it follows the information flow needed for assembly and is placed in correct stage of assembly process;
- the procedure correctly defines steps, the sequence of assembly and position of critical components;
- details are explained using photographs which enhances procedure simplicity;
- procedure contains all the steps needed for proper assembly of the rotor to the shaft;
- The procedure is mature as it is used unchanged since the EPX pump introduction.

The procedure contains all the information and is sufficient for proper assembly.

5.1.2 Assembly procedure not understood

Assembly process is carried out by 3 operators who alternate in the position according to production demand. All 3 operators were interviewed and their understanding of the procedure was checked.

All of them demonstrated good understanding and adherence to the assembly procedure.

5.1.3 Operator

The time spent on the shaft/rotor assembly position is estimated to be split between operators in ratio 75:20:5. Two faults discussed in this thesis are split between two operators. Distribution of the faults before was not recorded thus cannot be evaluated.

As it was shown above the assembly procedure is correct and its understanding by operators was confirmed. For that reason it is believed the occurrence of rejects is distributed evenly among all three operators although this cannot be 100 % proven at this moment.

5.2 Tooling

The nut is tightened on the shaft using torque control method.

Calibrated torque wrenches are used to carry out this step. 3 pieces of the wrench with valid calibration (valid for 1 year and expiring May 2016) are available at the assembly line (Figure 25). In order to evaluate the reliability and the precision of the torque set in these wrenches all of them were checked using TruCheck Plus torque tester.

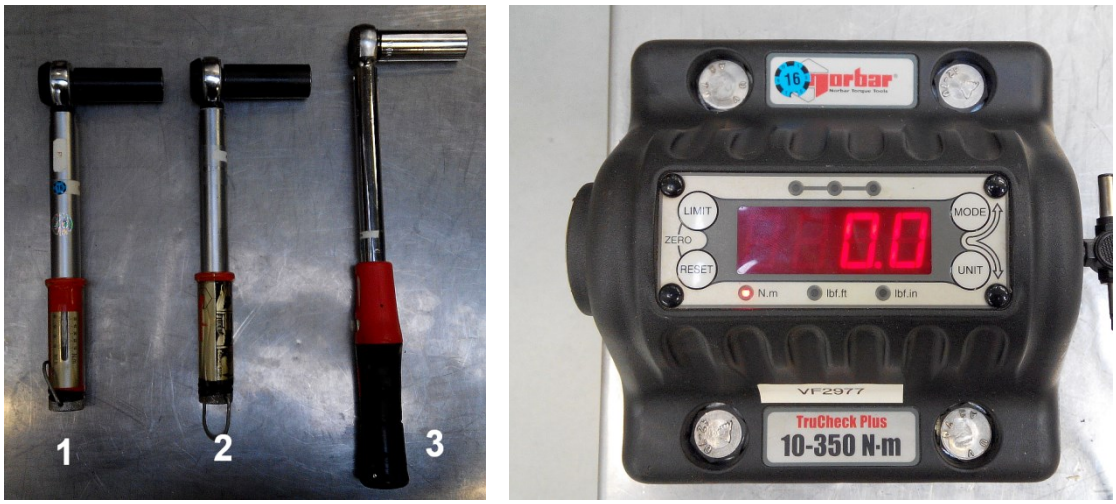

Figure 25: Torque wrenches and TruCheck Plus

The following Table 4 shows the values of torque found for wrenches used. Target value is 45 N.m:

Torque wrench number	Torque found (N.m)
1	45.3
2	44.0
3	45.7

Table 4: Torque values for wrenches used

It confirms that wrenches are set properly with minor spread which can be neglected.

5.3 The shaft thread and neck design

The following chapters deal with the thread and neck design especially with respect to the preload for a given torque.

5.3.1 Calculation of the preload force

The following Table 5 summarizes variables, units and absolute numbers used for calculation of the preload force $\boldsymbol{F}$.

The calculation was carried out using Equation 3:

Symbol	Name	Unit	Value	Note
T	Torque	N.m	45	Applied
d_2	Pitch diameter of the thread	m	0.009026	Values according to metric screw threads standard ISO 724
d_3	Minor diameter of the thread	m	0.00816	
P	Pitch of the thread	m	0.0015	
d_K	Shaft neck diameter	m	0.0079	Lower tolerance
μ_T	Thread friction coefficient		0.12 - 0.18	From [17]
μ_U	Undernut friction coefficient		0.1 - 0.18	From [17]
D_f	Effective frict. diameter nut	m	0.0155	

Table 5: Variables and their values used for preload force *F* calculation

The friction coefficients can be found in various literature sources like [18]. However, the spread in their values is significant and varies largely from source to source. The friction coefficient values used in this calculation are the lowest found for steel-steel combination not lubricated which means that the highest possible torque was transferred into a bolt preload. Lubrication decreases the friction so the load to the bolt can increase by 10 % (calculated using friction coefficients in [17]).

The calculated preload forces *F* for mutual combinations of friction coefficients are summarized in the following Table 6:

Preload force F [N]		μ_U	
		0.10	0.18
μ_T	0.12	27464	19925
	0.18	23065	17503

Table 6: Preload force F for given friction coefficients

5.3.2 Design of the shaft thread

As mentioned in Chapter 4.2.3.2, the thread used in case of EPX shaft is a standard M10x1.5-6g left-hand thread. When using preload force calculated above and Equation 4 combined with Equation 6, which was used for the calculation of effective section of the thread (A_T = 5.8 x 10^{-5} m^2), the following tensile stresses in thread σ_T for given friction coefficients can be calculated (Table 7):

Tensile stress σ_T [MPa]		μ_U	
		0.10	0.18
μ_T	0.12	473	343
	0.18	397	301

Table 7: Tensile stress in the shaft thread

The calculated tensile stress values in the thread σ_T are below the maximum stress allowed for the shaft material (453 MPa, see Chapter 4.2.3.1) but for the combination of lowest friction coefficients where the calculated stress is about 4% above the maximum.

The size of the thread was designed at the limit of material performance for the chosen safety factor.

5.3.3 Design of the neck

As visible from Figure 19 the diameter of the shaft neck can be anywhere between 7.9-8.1 mm. Using lower tolerance value 7.9 mm and combining Equation 5 with Equation 7 which was used for calculation of effective section of the neck (A_K = 4.9 x 10^{-5} m^2), the following tensile stress in the neck σ_K for given friction coefficient combinations can be calculated (Table 8):

Tensile stress σ_K [MPa]		μ_U	
		0.10	0.18
μ_T	0.12	560	406
	0.18	470	357

Table 8: Tensile stress in the shaft neck

The calculated tensile stress values in the neck σ_K are for some combinations of friction coefficients significantly higher than the maximum stress allowed for the shaft material (453 MPa, see Chapter 4.2.3.1). In the worst case the calculated stress can be higher by 24% which consumes most of the safety margin created by the safety factor used for calculation and makes a significant risk of shaft neck fracture especially when other unfavorable conditions are present.

The size of the undercut seems to be underdesigned for the given material and for some combinations of considered friction coefficients.

5.4 Shaft samples investigated

The sample set of the EPX shafts which was investigated consisted of 4 shafts with the following parameters:

1) Shaft thread broken during tightening before reaching 45 N.m torque. Only thread was left, the rest of the shaft was provided back to a supplier.
2) Shaft thread broken during tightening before reaching 45 N.m torque. The whole shaft was left for investigation.
3) Shaft thread which withstood intentional attempt for shaft fracture by application of torque ~ 100 N.m.
4) Shaft thread before any nut assembly and tightening - not used.

The main interest was focused on the samples 1 and 2 to find the cause of the fracture. Samples 3 and 4 were added for comparison and further material investigations. Where

applicable the threads were cut off well under the neck section for easier manipulation and investigation. The pictures of the threads available can be found in Table 9 below:

Sample 1	**Sample 2**	**Sample 3**	**Sample 4**

Table 9: Investigated samples overview

The following chapters describe the investigation and evaluation of these samples.

5.4.1 Thread dimensions

The dimensions of the sample threads were evaluated using good and fault reference thread gage for given thread 10x1.5 6g. The gages are shown in the picture (Figure 26):

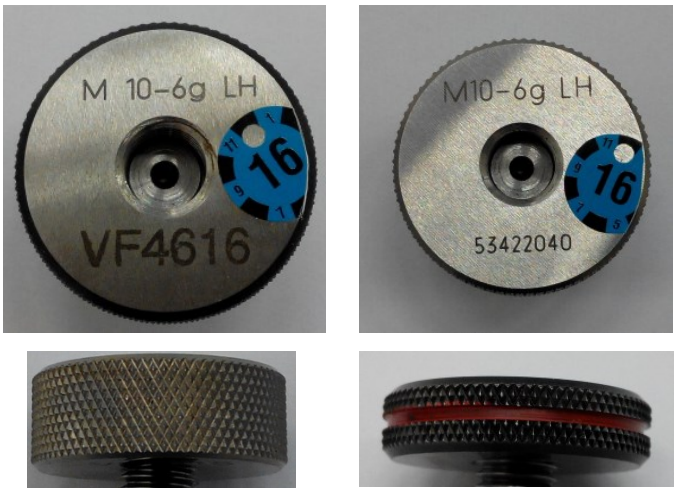

Figure 26: Good and faulty reference thread gages

The following table summarizes the results found = possibility to mount the gage to the thread (Table 10).

	Sample 1	Sample 2	Sample 3	Sample 4	10 unused	5 after mounting
Good gage	Not possible	Not possible	Possible with difficulties	Possible	Possible	Possible with difficulties
Fault gage	Not possible	Not possible	Not possible	Not possible	Not possible	Not possible
Nut	Possible	Possible	Possible	Possible	Possible	Possible

Table 10: The evaluation of shaft threads with reference gages and a nut

Note: 10 unused shafts and 5 shafts mounted in pumps were randomly selected for comparison. Mounting of gage to samples 1 and 2 could have been influenced by a bad grip of tested part.

It is shown that unused shaft threads can accommodate good reference gages. The threads already used for nut mounting could also accommodate the good reference gage but with difficulty esp. at lower part of the thread where the stress is always the highest. This can serve as an evidence of some plastic deformation in the thread after assembly torque application. However while precisely manufactured gage have difficulties with used threads the nut used in production fits all tested population well which shows the deformation after mounting is very small.

5.4.2 Undercut shape

As described in Chapter 4.2.3.5 the correct manufacturing of undercut is important for cracking initiation prevention.

EPX shaft is designed with undercut 1.5 which refers to the pitch of M10 thread. According to the design rules [13] the radii which are most important in preventing stress concentration should be 0.75 mm.

The profiles found for each sample are shown in Table 11:

Sample 1	Sample 2
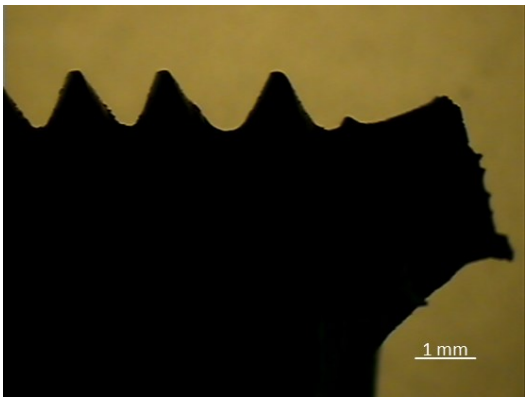	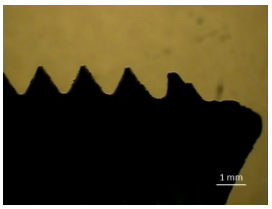 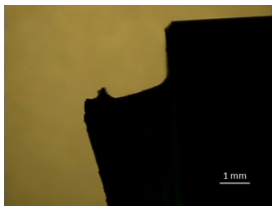 Left side on the neck Right side of the neck
Sample 3	**Sample 4**
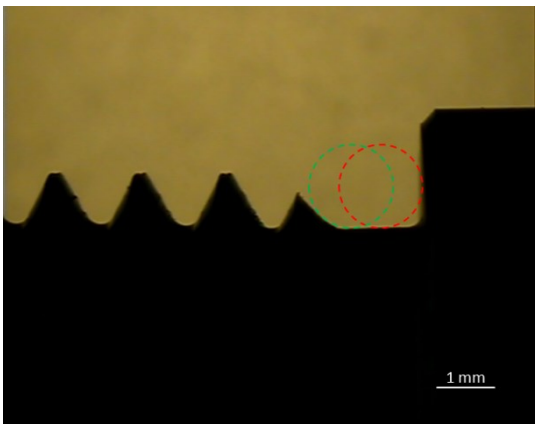	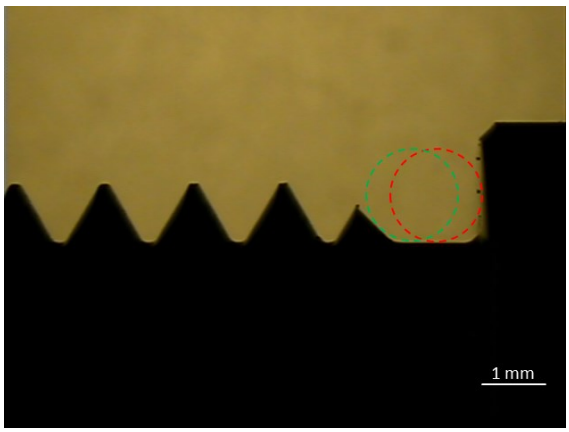

Table 11: Undercut shape investigation on studied samples

The undercut of the sample 1 could not be evaluated as the rest of the shaft was returned to the supplier.

Sample 2 was difficult to evaluate due to the neck fracture and related parts deformation however no sharp edges or shapes were visible and the corner on the right side of the neck was rounded (undercut radius was present).

In order to evaluate the shape of undercut auxiliary circles with required diameter 1.5 mm are shown in pictures. It was visible in both samples 3 and 4 which showed that the shape of the undercut deviated from the shape prescribed by drawing on the shaft side (red circle) while thread side appeared to be matching proper shape (green circle). All visible corners were round and there were no sharp edges.

Random selection of 5 shafts from current production showed similar issue as in Samples 3 and 4 which suggest this can be a standard feature throughout the whole EPX shaft population which comes from the shaft supplier.

Closer investigation of Sample 2 shaft revealed cracks in undercut radius which confirms smaller radii can weaken the material in this region (Figure 27).

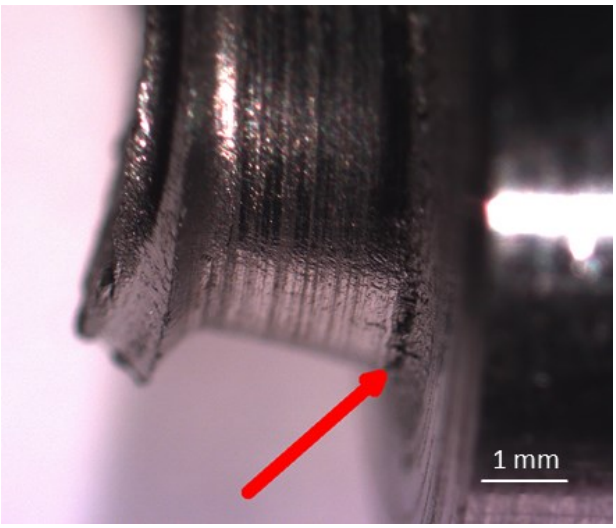

Figure 27: Comparison of undercut of EPX shaft

Summing up, the shape of the undercut on samples is different from what is defined in the shaft drawing (Figure 19) and can be considered a potential factor to the shaft fracture.

5.4.3 Cracks in material due to incorrect manufacturing

All samples were inspected in order to find possible cracks from manufacturing which could initiate shaft fracture.

Samples 3 and 4 showed no cracks both in undercut and in thread roots. Sample 3 thread showed some scratches which could have been accounted for overloading the thread during testing. Sample 4 showed only very small defects in shafts thread which were visible under electron microscope only (Table 12).

Sample 3	Sample 4
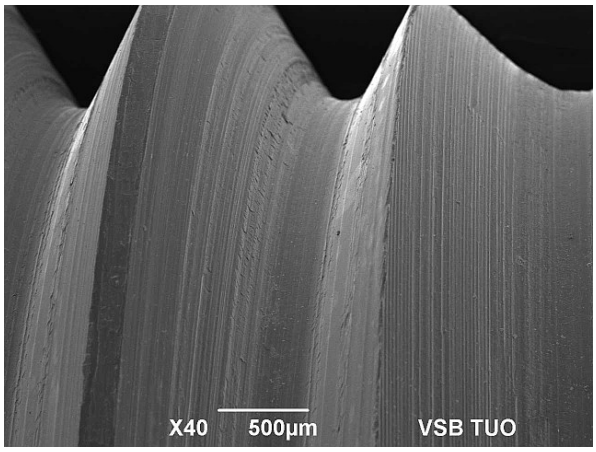	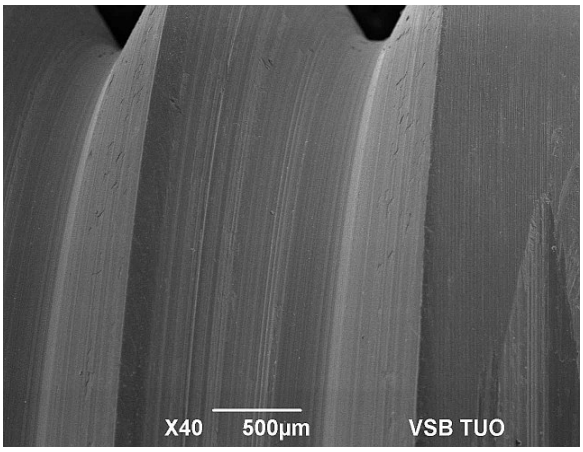
Sample 3	**Sample 4**
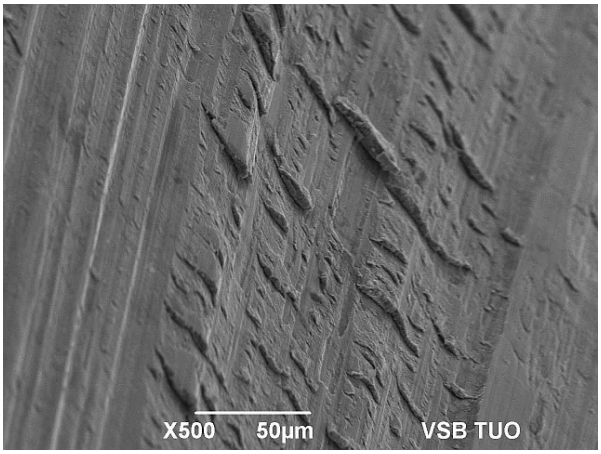	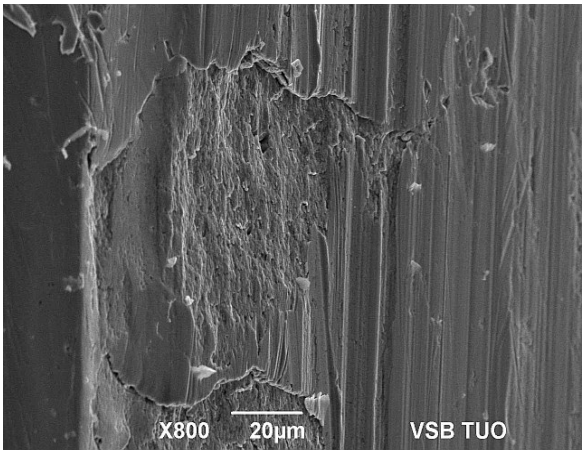

Table 12: Details of shaft threads of Samples 3 and 4

Samples 1 and 2 showed however big cracks in thread roots. Especially first turn root on both samples showed significant crack. This can be related to the load distribution among thread turns and shows the material was weakened there. Pictures also show that the whole thread was stretched and behaved like a test specimen in static tensile test (Table 13).

Sample 1	Sample 1 (detail)
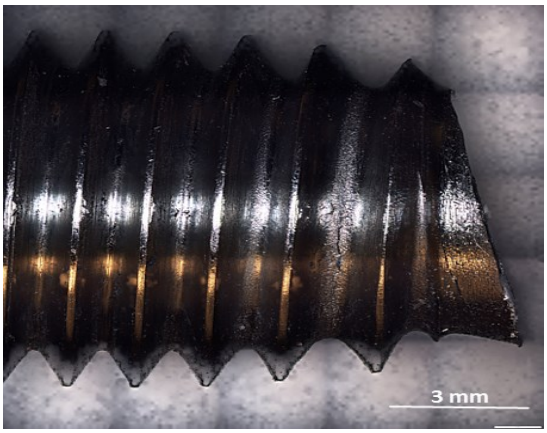	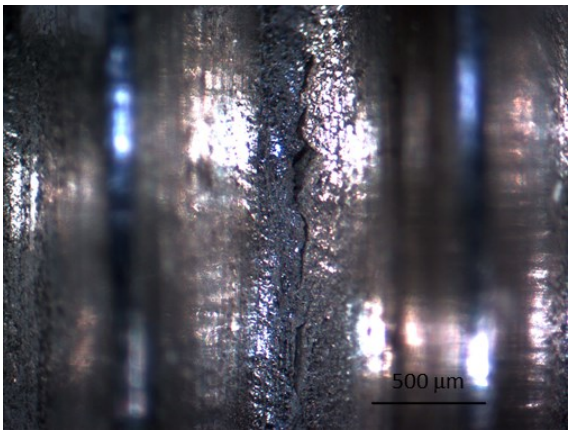

Table 13: Cracks in thread root of Sample 1

5.4.4 Shaft material investigation

Material used for shaft manufacturing has been described in Chapter 4.2.4. In order to check the designed properties of the material the following testing was done:

Tensile testing

Metallographic analysis

Fractography

5.4.4.1 Tensile testing

First test specimen per sample was made from the center of the shaft rest. The purpose of this arrangement was to investigate the material properties from the shaft center where segregation centerline could influence the material properties.

Second test specimen per sample was made from the same shaft piece but its position was close to surface. The approximate positions of samples are shown in the following picture (Figure 28):

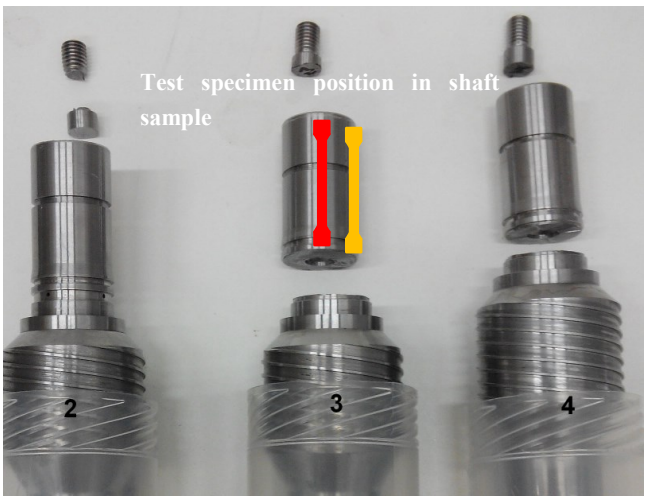

Figure 28: Tensile testing specimen approximate position in shaft samples

The results from the testing are described in Table 14. The data from material certificates from August 2014 and August 2015 supplied by the supplier are added to the table for comparison of material stability over time.

The results show a spread between the sample properties in tensile R_m, yield strength R_e and proof strength $R_p0.2$ parameters and also in elongation at fracture $A5$ which can indicate problems with raw material properties stability. While Sample 4 and material from August 2015 appear to be very close to the lower limit for tensile strength R_m, the yield strength R_e and proof strength $R_p0.2$ are significantly above specified values. The lowest value of $R_p0.2$ was measured in Sample 2 which was fractured thread.

None of the material samples is considered to be outside material specification described in Chapter 4.2.4 (considering there is no available information on the measurement repeatability).

	R_m [MPa]	R_e [MPa]	R_p 0.2 [MPa]	A5 [%]	Z [%]	Impact KV [J]	Brinnel hardness [HB]
2 center	886	-	725	18.7	63.8	-	-
2 side	902	-	732	19.3	63.8	-	-
3 center	933	-	768	18.7	59.6	-	-
3 side	922	-	764	21.3	63.8	-	-
4 center	844	-	808	13.3	55.6	-	-
4 side	849	-	809	14.7	63.8	-	-
Aug 2014	972	947	-	18.0	-	96	285
Aug 2015	856	824	-	19.0	-	86	255

Table 14: Tensile testing properties of the shaft material samples

R_e and R_p values are in some cases significantly higher than specification (680 MPa and 665 MPa respectively) which builds in additional safety by increasing maximum tensile stress level the thread and the neck can withstand.

5.4.4.2 Metallographic analysis

Samples 2, 3 and 4 were evaluated for presence on non-metallic inclusions and the presence of segregation and for microstructure to evaluate heat treatment (quenching and tempering).

Investigation of polished specimen revealed that Sample 2 suffered from significant presence of various non-metallic inclusions. The pictures in Table 15 below show Sample 2 and Sample 3. A significant difference can be seen as Sample 2 contains significant amount of sulphide inclusions (1), oxide inclusions (2) and a small piece of carbonitride of Niobium or Titanium (3). Contrary to that Sample 3 contains significantly less of sulphide inclusions but bigger oxide inclusion.

Sample 2	Sample 3
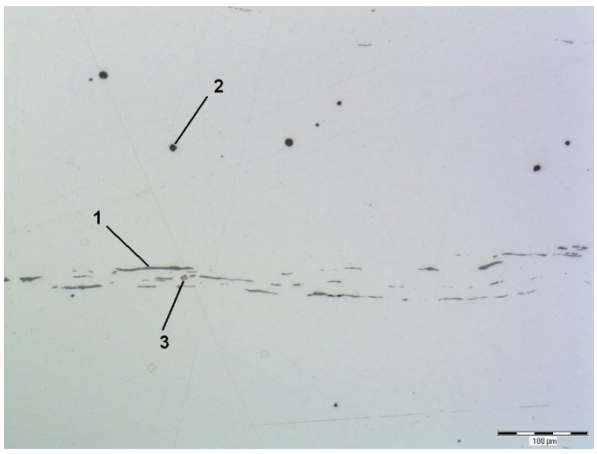	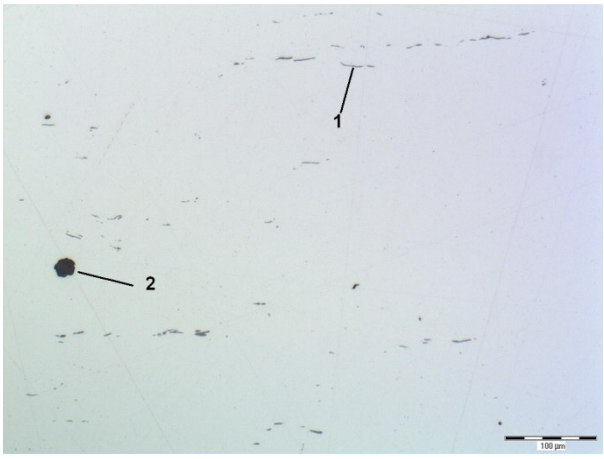

Table 15: Non-metallic inclusions - comparison of Samples 2 and 3

The presence of sulphide inclusions contributes to a presence of segregation line as described in Chapter 4.2.4.2. Such segregation could cause significant material strength deterioration which could contribute to the fracture of Sample 2 while Sample 3 survived even higher loading. The effect could have been local only as tensile testing of Sample 2 did not show any significant difference in material properties between center and side.

Sample 4 showed also sulphide inclusions in amount between Sample 2 and 3.

Samples after etching (Table 16) showed a fine sorbite structure of quenched and tempered steel which indicated the heat treatment was done correctly according the prescribed parameters.

Segregation (1) was again visible especially in Samples 2 and 4.

Sample 2 (mag. 50x)	Sample 3 (mag. 50x)
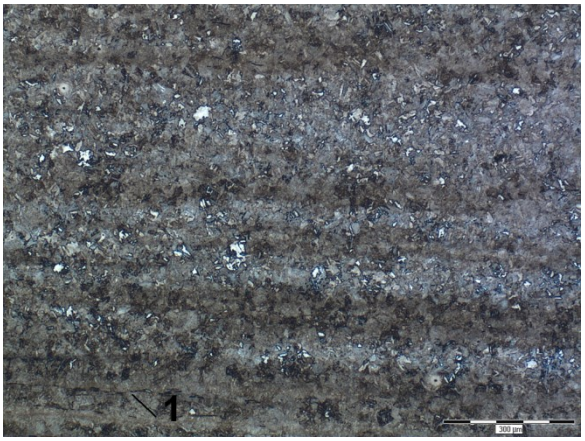	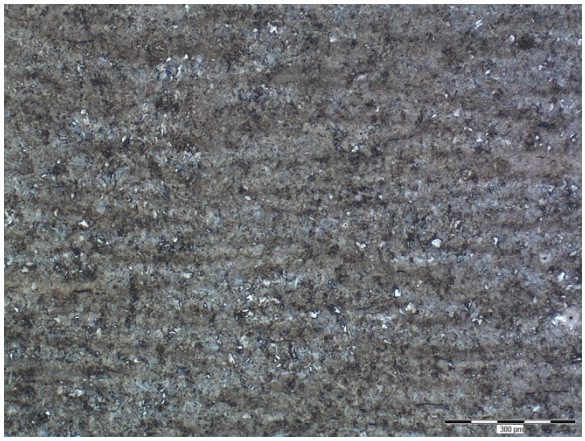
Sample 4 (mag. 50x)	**Sample 2 (mag. 500x)**
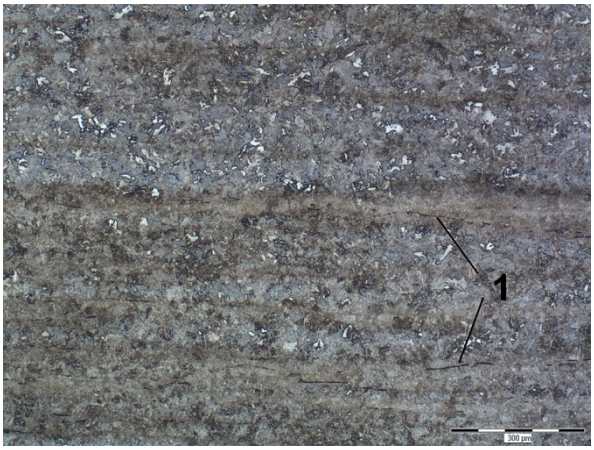	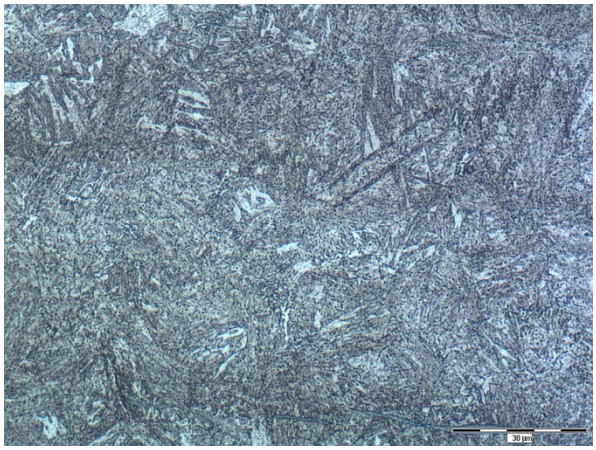

Table 16: Samples 2, 3 and 4 showing microstructure after etching

5.4.4.3 Fractography

Fractured threads from Samples 1 and 2 were investigated using scanning electron microscopy.

The pictures in Table 17 show the morphology of fracture area of Sample 1 only as both samples were comparable in appearance and properties.

Sample 1 overview	Sample 1 detail
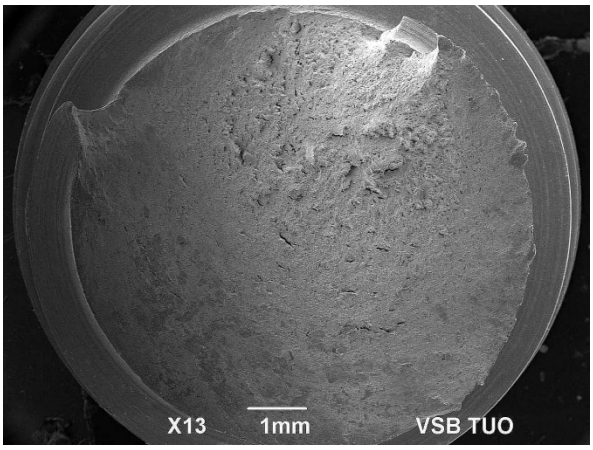	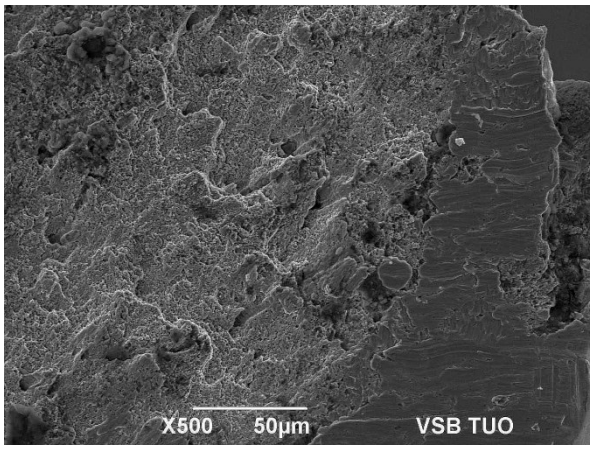
Sample 1 inclusions	**Sample 1 morphology**
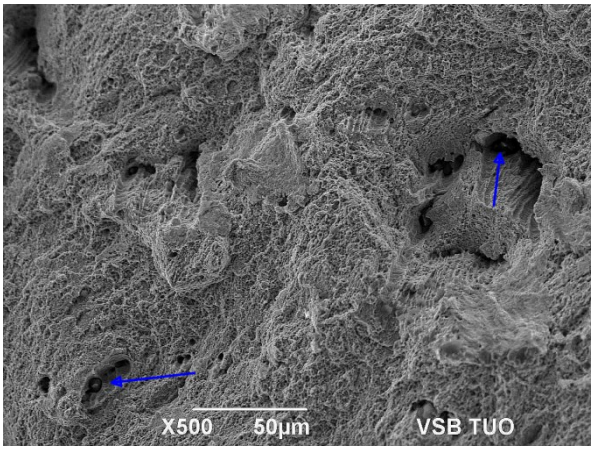	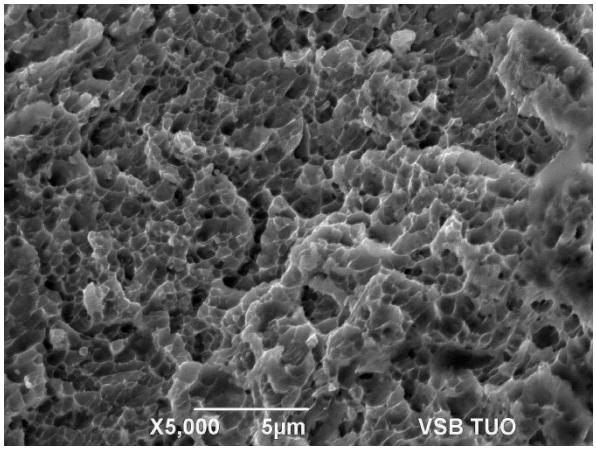

Table 17: Sample 1 fracture evaluation

Top left picture shows the overview of the whole fracture area.

Top right picture shows a detail of fracture where significant sliding areas can be recognized on the right side of the picture. Such area originated from sliding both pieces of shaft on top of each other at a terminal phase of the fracture process.

Bottom left picture shows detail of big dimples associated probably with non-metallic inclusions which could cause deterioration of material properties thus shaft fracture.

Bottom right picture shows a detail of fracture which was classified as transgranular ductile fracture with dimple morphology. The dimples are very fine and uniform which shows the heat treatment was done correctly.

6 Summary and discussion

The following chapter contains summary of the investigation findings and discusses the results.

6.1 Summary

Based on the investigation presented in Chapter 5 the following summary can be made:

1) The assembly procedure was found up to date, correct and clear, containing all steps needed for proper assembly.
2) Operators demonstrated good understanding and adherence to the assembly procedure.
3) Reject occurrence was distributed at least between 2 out of 3 operators. Older records are not available, thus higher occurrence of rejects with one operator cannot be confirmed nor rejected.
4) Tooling used for assembly possesses a valid calibration and checking of torque set did not show a significant deviation from set value 45 N.m.
5) The size of the thread was designed at the limit of material performance which makes a risk for a potential failure.
6) The thread neck due to its diameter showed that its design is even more critical than in case of the thread. The most unfavorable combination of friction coefficients showed the torque used can overload the thread neck almost by 25%.
7) Manufacturing dimensions of the thread are correct. It is slightly deformed during assembly by nut tightening however it does not create a problem with further assembly steps.
8) The undercut shape is not obeyed on samples which were not broken. As the same shape was seen also on other standard production shafts it is believed that this feature can increase susceptibility for shaft fracture occurrence which was demonstrated by a crack on Sample 2 which lay in undercut radius.
9) No cracks were seen both in the neck and the thread on non-fractured samples. However both fractured samples showed a significant crack in the first thread root from undercut which indicated the thread was weakened and thus overloaded.
10) Tensile testing showed fluctuation in material properties from sample to sample. Also certificates supplied by supplier showed changes of material properties in time. All samples fulfil the specifications (although Sample 4 is at the lower limit of the specification) but stability could be improved.
11) Metallographic analysis showed good microstructure of the material thus good heat treatment.
12) All samples suffer from non-metallic inclusions, especially the centerline segregation of sulphide inclusions. This segregation is the most visible in fractured Sample 2 where it creates significant line which could influence locally the material strength.

13) Fractography investigation classified the fracture as transgranular ductile fracture with dimple morphology. The dimples are very fine and uniform which confirms the heat treatment was done correctly.

Closer fracture area investigation revealed a presence of non-metallic inclusions.

6.2 Conclusion and recommendations

Based on the finding summarized in Chapter 6.1 the following can be concluded:

1) There was no single and unambiguous cause for shaft fracture found. The fault mechanism rather consists of synergic effect of 2 or more smaller issues which probably could not cause the shaft fracture individually but their combination could result in the fault occurrence.
2) In order to prevent shaft fracture and make the critical arrangement more robust the following recommendations could be made (arranged based on implementation simplicity):
    a. **The tightening torque decrease** – this would be the easiest solution how to improve robustness. For the combination of lowest friction coefficients and safety factor 1.5 the new torque value should be about 35 N.m. However a review with a designer must precede this step. More to that the reliability and spread in preload force can be improved by implementing angle-driven tightening.
    b. **Keeping the thread and washer free of lubricants -** lubrication decreases friction significantly thus higher preload forces can be accidentally achieved (3) which is critical for the shaft neck.
    c. **Improvement of material strength** – the use of material with a higher R_e value. Comparable materials to the currently used 817M40 are prescribed in BS EN 10277-5:2008 norm which supersedes old norm BS 970-3:1991 where 817M40 is defined. The new materials like 1.6582 or 34CrNiMo6 with minimum defined R_e value 800 MPa.
    d. **Increase of shaft thread diameter from M10 to M12** – this could lead to the increase of shaft neck diameter thus the improvement in allowed maximum stress by 60%. The change would require also change in the nut size, while the rest of the parts could stay the same.
    e. **Improvement of undercut manufacturing** – improvement and increase of radii to a required level should improve robustness under current conditions.

7 Experimental

The tensile testing was carried out by Materiálový a metalurgický výzkum s.r.o in Vítkovice using available shaft rests from the samples 2, 3 and 4. The usable part of each shaft was used to prepare test specimens with a diameter of 3 mm, measured length of 15 mm. The specimens were tested on MTS Landmark 100 kN at a speed of 0.4 mm/min, deformation was recorded using extensometer.

The undercut shapes of discussed samples were investigated using QuickScope QS-LZB machine by Mitutoyo.

Macroscopic pictures were made using laser scanning microscope Olympus LEXT 4100.

Metallography investigation was performed on tensile specimen heads using inverse metallographic microscope Olympus IX 70. Polished samples were used for non-metallic inclusions evaluation; etched samples were evaluated for microstructure (etching by Nital 2% - solution of nitric acid in ethyl alcohol).

Fractography was investigated using scanning electron microscope JEOL JSM-6490LV with secondary electrons imaging.

8 References

1. **Various authors.** *Edwards internal materials.* 2002-2016.
2. **Holweck, M. and Hebd, C. R.** *Seances Acad. Sci.* 1923, Vol. 177, p. 43.
3. **Chew, A. D., et al., et al.** Towards the single pump solution: Recent development in high speed machines for dry vacuum pumping. *J. Vac. Sci. Technol.* 2005, Vol. A 23(5).
4. **Helmer, J. C.** *J. Vac. Sci. Technol. A.* 1995, Vol. 13, p. 25.
5. **Chew, A. D.** A single pumping mechanism for high vacuum. *Vakuum in Forschung und Praxis.* 2012, Vol. 24, 2, pp. 26-30.
6. **Edwards.** *Edwards product catalogue.* 2014.
7. **Ishikawa, K.** *Introduction to Quality Control.* Tokio : 3A Corporation, 1990. SBN 4-906224-61-X.
8. **Wikipedia.** Seven Basic Tools of Quality. *Wikipedia.* [Online] 2016. https://en.wikipedia.org/wiki/Seven_Basic_Tools_of_Quality.
9. **VDI.** Systematic calculation of highly stressed bolted joints - Joints with one cylindrical bolt. *VDI 2230 Blatt 1:2015-11.* Berlin : VDI-Gesellschaft Entwicklung Konstruktion Vertrieb, 2003.
10. Screw thread design. [Online] Fastenal Company, 2016. https://www.fastenal.com/en/78/screw-thread-design.
11. Factors of safety. *The Engineering ToolBox.* [Online] 2015. http://www.engineeringtoolbox.com/factors-safety-fos-d_1624.html.
12. Torque Tightening. *Enerpac.* [Online] 2016. http://www.enerpac.com/en/torque-tightening.
13. **Maitra, G. M.** *Handbook of mechanical design.* New Delhi : Tata McGraw Hill Publishing, 2009. p. 6.2. 978-0-07-460238-6.
14. Wrought steel for mechanical and allied engineering purposes. *British Standard BS 970-3:1991.* London : BSI, 1991. 6. ISBN 0-580-1-9999-1.
15. **KV Steel Services.** EN24 and EN24T Steel. *KV Steel Services.* [Online] 2015. http://www.kvsteel.co.uk/steel/EN24T.html.
16. **Beckermann, C.** Macrosegregation. *ASM Handbook 15: Casting.* Novelty : ASM International, 2008, pp. 348-352.
17. **Beardmore, R.** Friction factors. *RoyMech.* [Online] 1 31, 2013. http://rommet.com/remco/misc/friction.htm.
18. **Oberg, E.** *Machinery's handbook.* New York : Industrial Press, 2012, p. 1525.